# The NLRP3 inflammasome is released as a particulate danger signal that amplifies the inflammatory response

Alberto Baroja-Mazo[1‡], Fatima Martín-Sánchez[1‡], Ana I. Gomez[1], Carlos M. Martínez[1], Joaquín Amores-Iniesta[1], Vincent Compan[2]*, Maria Barberà-Cremades[1], Jordi Yagüe[3], Estibaliz Ruiz-Ortiz[3], Jordi Antón[4], Segundo Buján[5], Isabelle Couillin[6], David Brough[2], Juan I. Arostegui[3], Pablo Pelegrín[1,2]

[1]Inflammation and Experimental Surgery Unit, CIBERehd, Institute for Bio-Health Research of Murcia (IMIB), Clinical University Hospital Virgen de la Arrixaca, Murcia, Spain

[2]Faculty of Life Sciences, University of Manchester, Manchester, UK

[3]Department of Immunology-CDB, Hospital Clinic, Barcelona, Spain

[4]Reumathology Pediatric Unit, Hospital Sant Joan de Deu, Barcelona, Spain

[5]Department of Internal Medicine, Hospital Vall d'Hebron, Barcelona, Spain

[6]Experimental and Molecular Immunology and Neurogenetics, CNRS UMR 7355, University of Orleans, Orleans, France

[‡]Equal contribution

*Present address: Department of Cell Biology, University of Geneva, Switzerland.

**Contact:** Dr. Pablo Pelegrín, Inflammation and Experimental Surgery Unit, Clinical University Hospital Virgen de la Arrixaca, Carretera Madrid Cartagena s/n, 30120 Murcia, Spain. Tel: +34 968 369 317; Fax: +34 968 920 532;

e-mail: pablo.pelegrin@ffis.es

**Running Title:** Extracellular function of the inflammasome

**Abstract**

NLRP3 inflammasome assembly activates caspase-1 and mediates the processing and release of the leaderless cytokine IL-1β, and thereby plays a central role in the inflammatory response and in diverse human diseases. Here we report that upon caspase-1 activation oligomerized NLRP3-inflammasome particles are released from macrophages. Recombinant oligomeric protein particles composed of the adapter protein ASC or the cryopyrin-associated periodic syndromes (CAPS) mutant NLRP3 p.D303N, stimulate further caspase-1 activation extracellularly, and also intracellularly upon phagocytosis by surrounding macrophages. ASC oligomeric particles were found in the serum of patients with active CAPS, but not in patients with other inherited autoinflammatory diseases. Our findings support a model whereby the NLRP3-inflammasome, acting as an extracellular oligomeric complex, amplifies the inflammatory response.

Inflammation is a tightly regulated response of the innate immune system against infection and tissue injury and aims to restore tissue homeostasis. Several soluble cytokines play crucial roles in this process including multiple inflammatory interleukins that lack a signal peptide such as IL-1β or IL-18[1]. Both cytokines are synthesized as inactive precursors and require post-translational processing by active caspase-1 to generate their mature active forms[1]. Caspase-1 activation is driven by the assembly of cytosolic multiprotein complexes named inflammasomes. Inflammasome complexes are composed of a sensor protein connected to caspase-1, an interaction that in most cases requires the adapter protein ASC (Apoptosis-associated Speck-like protein with a Caspase recruitment domain, encoded by *PYCARD*)[2]. Inflammasome-dependent caspase-1 activation is also required for the poorly understood unconventional release of IL-1β and IL-18[3]. Deregulated production of IL-1β underlies different human inflammatory diseases, including the inherited cryopyrin-associated periodic syndromes (CAPS), gout, atherosclerosis or type 2 diabetes[4,5,6,7].

The NLRP3-inflammasome is the most extensively studied inflammasome that is formed upon NLRP3 oligomerization and subsequent recruitment of ASC and pro-caspase-1[2]. Upon NLRP3 activation, ASC proteins assemble into fiber-like structures that culminate in the production of a large protein aggregate that enormously amplifies caspase-1 activation[8,9]. The NLRP3-inflammasome is activated in response to a variety of infectious stimuli, or to cellular stress caused by different sterile danger signals[2], including high concentrations of extracellular ATP, decrease of extracellular osmolarity or pH, monosodium urate (MSU) or cholesterol crystals, β-amyloid fibers, degradation of extracellular matrix components, vaccine adjuvants, and environmental or industrial particles and nanoparticles[6,7,10,11,12,13,14,15,16]. All these extracellular stimuli converge to activate the NLRP3-inflammasome through an

undefined mechanism, but which has been suggested to include a decrease of intracellular $K^+$, $Ca^{2+}$ signaling, production of reactive oxygen species (ROS), phagolysosomal membrane damage and the activity of cathepsins, release of oxidized mitochondrial DNA into the cytosol secondary to mitochondrial damage, TGF-β activated kinase 1 (TAK1) activity and deubiquitination[11,17,18,19,20,21,22].

In conjunction with the release of mature IL-1β and IL-18, inflammasome-dependent caspase-1 activation also controls the release of additional cytosolic proteins through an unconventional pathway that includes the release of alarmins such as high mobility group box 1 (HMGB1) protein[23,24]. The majority of reports studying caspase-1 maturation after inflammasome assembly found active caspase-1 subunits (p10 and p20) in cell supernatants[6,11,17,18,19,20,21,22,25,26]. These data suggest that caspase-1 may be regulating its own release. However, the (patho-)physiological role of extracellular caspase-1 and the inflammasome remains to be addressed.

Here, we report that NLRP3 and ASC inflammasome oligomeric particles were released together with IL-1β and the active caspase-1 subunits upon inflammasome activation. ASC oligomeric particles could activate caspase-1 extracellularly and in wild-type, *Pycard*$^{-/-}$ and *Nlrp3*$^{-/-}$ macrophages upon internalization, and therefore function as previously undescribed danger signals that spread inflammatory signaling to surrounding macrophages. Similarly, *NLRP3* mutations causative of human CAPS also caused formation of oligomeric particles that upon release from the cell became functional and were able to activate caspase-1 in both wild-type and *Nlrp3*$^{-/-}$ mouse macrophages. ASC oligomers were found in the serum of patients with active CAPS, but not in patients with the inherited autoinflammatory syndromes familial Mediterranean fever (FMF) or TNF receptor-associated periodic syndrome (TRAPS).

## RESULTS

### Inflammasome components are released upon NLRP3 activation

The activation of caspase-1 by the NLRP3-inflammasome is associated with the secretion of the leaderless cytokines IL-1β and IL-18 via an unconventional release pathway[3]. Examination of macrophage supernatants after NLRP3-inflammasome activation by ATP or nigericin resulted, as expected, in the release of mature IL-1β and the p10 subunit of caspase-1, but also in the inflammasome components NLRP3, ASC and pro-caspase-1 (p45) (**Fig. 1a**). Quantification of released protein relative to the total amount of intracellular protein revealed that after NLRP3 inflammasome activation the majority (> 50 %) of the protein pool for IL-1β, the p10 subunit of caspase-1 and ASC was found in the supernatant (**Supplementary Fig. 1a**). However, less than 50 % of pro-IL-1β, pro-caspase-1 (p45), NLRP3 or β-actin was extracellular (**Supplementary Fig. 1a**). Time-course experiments revealed that all inflammasome components (ASC, caspase-1, NLRP3, IL-1β) could be detected in the cell supernatant after 15 min of NLRP3-inflammasome stimulation (**Fig. 1b**). Full blots for intracellular proteins, extracellular IL-1β and caspase-1 revealed little mature IL-1β and p10 subunits remained associated with cell lysates (**Supplementary Fig. 1b**). Densitometry of extracellular proteins during the time-course of NLRP3-inflammasome stimulation demonstrated that the kinetics for the release of inflammasome components was similar during the first 30 min, then NLRP3 release was delayed when compared to IL-1β, the p10 subunit of caspase-1 and ASC (**Fig. 1c**). Prolonged activation of the inflammasome results in a specific type of cell death called pyroptosis, characterized by a loss of plasma membrane integrity and the late release of intracellular proteins, including the cytosolic enzyme lactate dehydrogenase (LDH)[27]. To investigate whether the release of inflammasome

components could be associated with pyroptosis, we measured the presence of LDH in cell supernatants, and the permeability of the plasma membrane to small molecules. NLRP3 activation for 30 min resulted in levels of LDH release below 25 % of the total cellular LDH content, while the majority of cells presented a plasma membrane permeable to YoPro-1 (MW 629 Da) (**Fig. 1d**). LDH release then increased over the period of stimulation reaching > 50% of the total cellular LDH after 2 h of stimulation (**Fig. 1d**). This shows that upon NLRP3 inflammasome activation, NLRP3 and ASC proteins are found extracellularly at early time points, together with pro-inflammatory IL-1β cytokine.

We next found that NLRP3-inflammasome activation by particles, and the activation of NLRP1- or AIM2-inflammasomes, also lead to the release of ASC, NLRP3, IL-1β, and the p10 subunit of caspase-1 (**Fig. 1e**). In contrast NLRC4 activation did not result in NLRP3 protein release, but other inflammasome proteins were found extracellularly (**Fig. 1e**). All these treatments resulted in increased release of LDH, from 25 to 50 % of the total cellular content (**Supplementary Fig. 1c**).

Upon inflammasome activation, NLRP3 release was maintained after caspase-1 inhibition, and from ASC and Caspase-1/11 double-deficient (*Casp1*$^{-/-}$*Casp11*$^{-/-}$) macrophages (**Fig. 1f**, full immunoblots for extracellular IL-1β, caspase-1 and β-actin can be found in **Supplementary Fig. 1f**). Quantification of released protein by densitometry showed a 16.3 % reduction in NLRP3 release after caspase-1 inhibition, and a decrease in release of 88.3 % for ASC (**Supplementary Fig. 1d**). ATP activation of inflammasome knock-out macrophages did not result in a significant change in the release of LDH (**Supplementary Fig. 1e**). All these data suggest that the majority of NLRP3 is passively released after a sustained stimulation, whereas ASC release occurred quickly and was highly dependent on caspase-1 activity.

**Extracellular inflammasomes are oligomeric particles**

We found that after 10-30 min of NLRP3-inflammasome activation, extracellular ASC was oligomeric as revealed by crosslinking experiments (**Fig. 2a** and **Supplementary Fig. 2a**). Extracellular ASC from ATP-activated macrophages co-immunoprecipitated with NLRP3 (**Fig. 2b**), suggesting that NLRP3 and ASC could form oligomeric inflammasome particles extracellularly. By using time-lapse microscopy of nigericin-treated macrophages expressing ASC-mCherry, we found that following intracellular ASC oligomerization, the ASC speck was released after 5 min (**Supplemental Video 1**). Extracellular ASC specks could be also detected by immunofluorescence staining for ASC in macrophages activated with ATP (**Fig. 2c**). In these preparations, staining cell membrane with cholera toxin B and F-actin cytoskeleton with phalloidin, revealed that some ASC specks are beyond the limit of the cell boundary (**Supplementary Fig. 2b**). We then quantified the number of ASC specks that were intracellular, close to the inner cell surface, and outside of the cell (**Fig. 2d**) and found that after 20 min of stimulation with ATP, most of the ASC specks were found extracellularly (58±15.5%), or close to the cell perimeter (24±12.8%) (**Fig. 2e**). Flow cytometry of cell-free supernatants from ATP-treated macrophages revealed extracellular inflammasome particles stained for ASC and NLRP3 (**Fig. 2f**). These particles appear to be close in size to 3 μm-calibrated beads as determined by flow cytometry (**Supplementary Fig. 2c**), however we could not exclude that particle aggregation occurred during the sample preparation. Specific staining for ASC and NLRP3 was confirmed by using supernatants from *Pycard*$^{-/-}$ or *Nlrp3*$^{-/-}$ macrophages (**Fig. 2g**). NLRP3 released upon inflammasome stimulation from ASC-deficient macrophages formed extracellular particles (**Fig. 2g**). However,

caspase-1 deficiency impaired the release of both ASC and NLRP3 oligomeric particles (**Fig. 2g**). These data suggest that the little release of NLRP3 in caspase-1 deficient macrophages detected by immunoblot (**Fig. 1f**) could represent a small fraction of soluble NLRP3 that could not form detectable specks, indicating that inflammasome oligomeric particles are highly released via caspase-1-dependent pyroptosis. Macrophages stimulated by different NLRP3 inducers, as well as for NLRP1, NLRC4 and AIM2, released significant amounts of ASC specks (**Supplementary Fig. 2d**). Confirming cross-linking experiments, extracellular inflammasome particles were found at early time points following NLRP3 stimulation (**Supplementary Fig. 2e**), and 54.06±7.82 % (*n*=11 independent experiments) of extracellular ASC particles detected by flow cytometry were also positive for NLRP3 staining. These data suggest that caspase-1 activation, probably by inducing pyroptosis, controls the release of oligomeric inflammasome particles composed of NLRP3 and the adapter protein ASC.

**Extracellular ASC specks activate the NLRP3 inflammasome**

We characterized caspase-1 activity in macrophage supernatants upon inflammasome activation, since the detection of the mature subunits of caspase-1 by immunoblot would not necessarily implicate that this extracellular caspase-1 is active, since potential association with inhibitors or inappropriate folding in a cell-free environment could result in inactive enzyme. Using the cleavage of the fluorescent specific substrate z-YVAD-AFC we found that macrophage supernatants presented between 5-8 Units of active caspase-1 (**Fig. 3a**). Extracellular caspase-1 activity after NLRP3-inflammasome stimulation was absent in *Nlrp3*$^{-/-}$ and *Pycard*$^{-/-}$ macrophages (**Fig. 3a**). Extracellular caspase-1 activity released from macrophages treated with

ATP or nigericin was able to process pro-IL-1β in a cell free environment in a manner similar to recombinant caspase-1 (**Fig. 3b**). We also found significant additional activation of caspase-1 over time when supernatants were incubated without cells after NLRP3-stimulation (**Fig. 3c**), indicating that extracellular inflammasome oligomers could process pro-caspase-1 in supernatants. This activation was absent in supernatants from *Nlrp3*$^{-/-}$ macrophages that do not release ASC or pro-caspase-1 upon stimulation (**Fig. 3c**).

To study the function of extracellular ASC particles, we produced and purified YFP fluorescent recombinant ASC oligomeric specks from HEK293 cells, made possible by the fact that transfection of ASC-YFP leads to spontaneous aggregation of ASC into a single speck (**Supplementary Fig. 3a**). Recombinant ASC-YFP particles appeared as fiber-like structures by fluorescence microscopy (**Fig. 3d**) and were gated in the same region as macrophage released-ASC specks when analyzed by flow cytometry based on FSC versus SSC parameters (**Supplementary Fig. 3b**). Previous reports have demonstrated that ASC polymerizes into a prion-like speck[8,9], and electron microscopy examination of recombinant ASC-YFP revealed large aggregates of fibers (**Fig. 3e**). This structure was similar to the speck identified by electron microscopy in macrophages treated with nigericin (**Fig. 3f** and **Supplementary Fig. 3c**) and revealed a fiber-like structure of approximately 2 μm in diameter. This size was similar to the one found for extracellular inflammasomes detected by flow cytometry (**Supplementary Fig. 2c**), and the size of inflammasome structures recently reported[9]. Electron microscopy analysis of macrophages with inflammasome-specks also revealed a separation of the cytoplasm, with approximately half of it well structured (with visible organelles and intact plasma membrane), and the rest of the cytoplasm completely vacuolized and destructured with numerous autophagy vesicles.

The inflammasome oligomeric speck was found in between, or in some cells, in the destructured part of the cytoplasm close to the cell edge, where plasma membrane integrity was compromised (**Fig. 3f** and **Supplementary Fig. 3c**). To further validate the functionality of recombinant ASC-YFP specks, we showed that they are able to nucleate soluble ASC-mCherry to form larger mixed ASC aggregates (**Fig. 3g**).

Addition of recombinant ASC-YFP oligomeric specks to cell-free supernatants from macrophages that had been previously activated with different concentrations of nigericin resulted in an increase of caspase-1 activity in supernatants obtained from wild-type, but not from *Nlrp3*$^{-/-}$ macrophages (**Fig. 3h**). The potentiation of caspase-1 activity by ASC-YFP oligomers in cell-free supernatants was abolished when a buffer with 150 mM KCl was used, or when ATP was degraded using apyrase (**Fig. 3i**). Addition of recombinant ASC-YFP oligomeric specks to macrophages together with ATP enhanced the release of IL-1β from wild-type and *Pycard*$^{-/-}$ macrophages, but not from *Nlrp3*$^{-/-}$ macrophages (**Fig. 3j** and **Supplementary Fig. 3d**). These data suggest that extracellular ASC oligomeric particles could rescue the deficiency of intracellular ASC in *Pycard*$^{-/-}$ macrophages during ATP stimulation. As a control, mock-transfected HEK293 cell lysate was subjected to the same purification protocol as for the ASC specks and the resulting product failed to induce the release of IL-1β from macrophages (**Fig. 3j**). Recombinant extracellular ASC-YFP specks were also able to restore caspase-1 activation in *Pycard*$^{-/-}$ macrophages following ATP stimulation, but not in *Nlrp3*$^{-/-}$ macrophages (**Supplementary Fig. 3f**). The potentiation effect of extracellular ASC-YFP oligomeric particles was more evident when incubated for 3 h together with suboptimal concentrations of ATP or MSU crystals (**Supplementary Fig. 3f**). In these experiments where cells were stimulated from 3 to 16 h, we found that recombinant ASC-YFP specks alone induced IL-1β

release (**Supplementary Fig. 3f**), and that the macrophages ingested ASC-YFP particles (**Fig. 4a**).

By increasing the ratio of recombinant ASC-YFP particles per macrophage we were able to increase IL-1β release over 3 h of incubation (**Fig. 4b**). In that situation, the release of IL-1β was independent of ASC and NLRP3, but was completely dependent on caspase-1 (**Fig. 4b**). Addition of recombinant ASC-YFP specks also increased caspase-1 activity in wild-type macrophages and to a lesser extent in *Nlrp3*$^{-/-}$ macrophages (**Fig. 4c**). Release of IL-1β induced by incubation with ASC-YFP was significantly inhibited when phagocytosis was blocked using cytochalasin B, or when the cathepsin B inhibitor Ca074 was applied, but not when high extracellular $K^+$, or when the anti-oxidant N-acetyl-L-cysteine (NAC) was used (**Fig. 4d**). As a control, purified preparations from mock-transfected HEK293 cells failed to induce the release of IL-1β from macrophages (**Fig. 4d**). Upon ASC-YFP particle internalization, macrophages with ingested ASC-YFP specks presented aggregates of caspase-1, similar to the ones found in ATP-activated macrophages (**Fig. 4e**). Intraperitoneal injection of ASC-YFP oligomeric particles into mice resulted in an increase in the number of peritoneal granulocytes recruited in wild-type mice, but not in *Casp1*$^{-/-}$*Casp11*$^{-/-}$ mice (**Fig. 4f**), and also increased the amount of IL-1β in the peritoneum of wild-type mice (**Fig. 4g**). Our data support a dual role for the extracellular ASC-speck in modulating caspase-1 activity. It can directly regulate caspase-1 in the extracellular environment, and also upon internalization by macrophages by directly nucleating and activating pro-caspase-1. In the latter case NLRP3 is not required when oligomeric ASC is internalized by macrophages.

**Extracellular p.D303N NLRP3 specks activate caspase-1**

To study the possible function of extracellular active NLRP3 particles, we generated constitutively-activated CAPS-associated *NLRP3* mutants and expressed them in HEK293 cells. The expression of different CAPS-associated *NLRP3* mutants (p.R260W, p.T348M and p.D303N), but not its wild-type version, in HEK293 cells resulted in the spontaneous self-oligomerization of mutated NLRP3 into specks (**Fig. 5a**). ATP-stimulation of HEK293 expressing both $P_2X_7$ receptor and p.D303N *NLRP3*-YFP released p.D303N NLRP3-YFP oligomeric particles into the cell supernatant, as was evident by fluorescence microscopy (**Fig. 5b**), flow cytometry analysis of cell supernatants (**Fig. 5c**), and by immunoblot (**Fig. 5d**). ATP treatment of HEK293 expressing the purinergic $P_2X_7$ receptor resulted in plasma membrane permeabilization to YoPro-1 and a significant increase in cell death, as assessed by LDH release (**Fig. 5e**). We next purified recombinant p.D303N NLRP3-YFP particles from HEK293 cells (**Fig. 5f**) and analyzed their ultrastructure by electron microscopy. Different from recombinant ASC-YFP specks, p.D303N NLRP3-YFP oligomeric particles appeared smaller in size, and as compact globular aggregates (**Fig. 5g**) that were able to aggregate ASC when co-expressed in HEK293 cells (**Fig. 5h**), similar to what has been recently proposed for the active NLRP3 heads that serve as scaffolding to oligomerize ASC fibers into a large particle[8,9].

To examine if p.D303N NLRP3-YFP oligomeric particles were extracellularly functional, we incubated them with cell-free supernatants from ATP-treated macrophages and found that p.D303N NLRP3-YFP particles co-localized with macrophage-released ASC (**Fig. 5i**), suggesting that they could nucleate extracellular ASC in a cell-free environment. This was further confirmed by fluorescence microscopy where p.D303N NLRP3-YFP oligomeric particles served as scaffolds to oligomerize soluble ASC (**Fig. 5j**).

Using immunofluorescence and immunoblot analysis of cell lysates, we found that macrophages were able to phagocyte recombinant p.D303N NLRP3-YFP particles (**Supplementary Fig. 4a,b**), without inducing significant cell death (**Supplementary Fig. 4c**). Addition of recombinant p.D303N NLRP3-YFP oligomeric particles to wild-type or *Nlrp3*$^{-/-}$ macrophage increased the release of IL-1β (**Fig. 6a,b**), activated caspase-1 (**Fig. 6c**) and induced the formation of endogenous ASC specks (**Fig. 6d,e**), with the subsequent release of ASC oligomeric particles as detected by flow cytometry (**Fig. 6f**). However, p.D303N NLRP3-YFP particles failed to induce IL-1β release and caspase-1 activation in *Pycard*$^{-/-}$ macrophages (**Fig. 6b,c**). These data suggest that extracellular particles with the gain-of-function p.D303N *NLRP3* mutation require ASC to activate caspase-1, as ASC is the adapter molecule that links NLRP3 oligomers to pro-caspase-1.

Phagocytosis of p.D303N NLRP3-YFP particles was observed in 33 % of macrophages containing ASC specks (**Supplementary Fig. 4d**). The blockade of p.D303N NLRP3-YFP particle internalization with cytochalasin B reduced IL-1β release by 69 % (**Fig. 6g**) and decreased the number of macrophages with ASC specks by 31 % (**Supplementary Fig. 4e**). Recombinant p.D303N NLRP3-YFP particles were able to induce IL-1β release from macrophages when a high extracellular $K^+$ buffer was used, or when the anti-oxidant NAC or the cathepsin B inhibitor Ca074 were used (**Fig. 6h**). These data show that intracellular $K^+$ efflux, ROS generation and cathepsin B activity required to form new NLRP3 aggregates, are not necessary when a macrophage internalizes a pre-assembled active NLRP3 particle. Intraperitoneal injection of p.D303N NLRP3-YFP recombinant specks into wild-type mice resulted in an marked increase in the number of peritoneal granulocytes (**Fig. 6i**), and increased production of IL-1β (**Fig. 6j**), that was absent in *Pycard*$^{-/-}$ mice (**Fig. 6i,j**).

Therefore, constitutively active NLRP3 proteins could self-oligomerize in the absence of the adapter protein ASC into particles that could be released from cells, and upon internalization by surrounding macrophages they are able to activate caspase-1 by recruiting ASC.

**Inflammasome particles in the serum of CAPS patients**

CAPS are a consequence of rare heterozygous, gain-of-function *NLRP3* mutations, and include three clinical phenotypes of increasing severity. These range from the least severe familial cold autoinflammatory syndrome (FCAS), to Muckle-Wells syndrome (MWS), and the chronic infantile neurological, cutaneous and articular syndrome (CINCA) being the most severe phenotype[28]. The data described above show that *NLRP3* gain-of-function mutants correlate with the aggregation of NLRP3 into particles with pro-inflammatory extracellular activity that induced the release of ASC specks. We therefore analyzed the presence of ASC and NLRP3 particles in the serum of patients with CAPS during a symptom-free interval, and during acute inflammatory episodes. Using fluorescence microscopy and flow cytometry, we discovered ASC particles in the serum of patients with all clinical phenotypes of CAPS (**Fig. 7a,b** and **Supplementary Table 1**). We then confirmed that the serum isolation protocol by centrifugation did not induce loss of inflammasome particles (**Supplementary Fig. 5a**) and that ASC-YFP recombinant particles were gated in the same area as that of inflammasome particles from CAPS patients based on FSC versus SSC parameters, which were adjusted to display a correct separation of leukocyte populations (**Supplementary Fig. 5b**).

Serum of patients with active CAPS presented pathological concentrations of C-reactive protein (CRP) > 10 mg/l (**Fig. 7c**) and a statistically significant increase in

extracellular ASC oligomeric particles (**Fig. 7d**). However, there were no significant differences in extracellular ASC particles in the serum of healthy donors compared with CAPS patients during symptom-free interval (CRP < 10 mg/l, **Fig. 7d**). Percentages of ASC particles present in the serum from healthy donors and from CAPS patients during symptom-free intervals were below background staining obtained for serum samples stained with secondary antibody alone. Among the different CAPS phenotypes, a clear tendency for high CRP values and a general tendency towards elevated amounts of extracellular ASC particles in the serum were detected (**Supplementary Fig. 5c,e**). In 8 out of the 14 patients analyzed with active CAPS, the percentage of extracellular NLRP3-positive particles in the serum was above the average of healthy donors and background staining was especially exacerbated in four patients (three with MWS and one CINCA) (**Fig. 7e** and **Supplementary Table 1**). However, increased NLRP3 particles in serum of the group of patients with active CAPS appeared to have no statistically significant difference compared to healthy donors (**Fig. 7e**). This increase was also not significant when the CAPS patients were stratified by clinical phenotypes (**Supplementary Fig. 5d**). From the seven patients with elevated detection of ASC and NLRP3 particles in serum, we found that 48.32±7.82 % of ASC specks were also positive for NLRP3, demonstrating that in CAPS patients there are particles double positive for ASC and NLRP3 with a similar ratio to that found in macrophage supernatants. We also evaluated the presence of ASC and NLRP3 particles in the serum of patients with other inherited autoinflammatory syndromes not related with *NLRP3* mutations. In particular, we examined patients with FMF, carrying biallelic *MEFV* mutations, and patients with TRAPS, carrying structural heterozygous *TNFRSF1A* mutations. Despite both groups of patients having increased amounts of serum CRP (**Fig. 7c**), they did not present a

statistically significant increase in serum ASC- or NLRP3-positive particles when compared with the group of healthy donors (**Fig. 7d,e**).

Among CAPS, there is a rare group of patients with low-level somatic *NLRP3* mosaicism that causes auto-inflammatory phenotypes. We analyzed the serum of four patients with a range of 9 to 31 % of somatic *NLRP3* mosaicism during active disease (**Supplementary Table 1**). We found that CAPS patients with somatic mosaicism presented statistically significant elevated amounts of ASC oligomeric particles in the serum (**Fig. 7d**), and two patients also presented elevated NLRP3 particles in the serum (**Fig. 7e**).

Although IL-1β is driving the clinical phenotype in CAPS, IL-1β was elevated only in some patients with CAPS, independently of their phenotype or serum CRP concentration (**Fig. 7f**, **Supplementary Fig. 5g** and **Supplementary Table 1**). Serum IL-1β levels were markedly variable among the different CAPS patients and we were unable to find any positive correlation with serum CRP level or with the presence of serum ASC- or NLRP3-positive particles (**Supplementary Fig. 5f**). The inflammatory cytokines IL-6 and TNF were also elevated in some patients with active CAPS (**Fig. 7f** and **Supplementary Table 1**) and presented a tendency to increase as the CAPS severity increased (**Supplementary Fig. 5g**). Taken together, these data suggest that the detection of ASC particles could represent a biomarker for active CAPS syndromes and could be involved in the pathophysiology of the disease by activating surrounding macrophages.

## DISCUSSION

In this study, we found that inflammasome activation led to the release of functional oligomeric inflammasome particles containing both NLRP3 and ASC that act as danger signals to amplify inflammation by promoting the activation of caspase-1 extracellularly and in surrounding macrophages following their internalization. Caspase-1 activity was necessary for the release of inflammasome particles from activated macrophages during pyroptosis. Released extracellular caspase-1 was active and able to maturate pro-IL-1β. Both ASC and the structural gain-of-function p.D303N *NLRP3* mutant associated to CAPS, oligomerized into active particles of different composition that were detected in the serum of patients with active CAPS syndromes.

Caspase-1 is a protease that controls the release of multiple leaderless proteins, including its own release[24]. The caspase-1 secretome in macrophages includes the well-studied pro-inflammatory cytokines IL-1β and IL-18, the alarmin HMGB1, as well as proteins that are not direct substrates of the protease, such as IL-1α or fibroblast growth factor (FGF)-2[23,24,29]. The proteins released upon caspase-1 activation are mainly involved in inflammation, cytoprotection and tissue repair[24]. The caspase-1 activating NLRP3-inflammasome controls the caspase-1 secretome, and here we have additionally found that caspase-1 controls the release of inflammasome oligomeric particles containing NLRP3 and ASC. This suggests an additional regulatory role for the inflammasome complex acting as an extracellular danger signal.

Caspase-1 induces a specific type of cell death in macrophages called pyroptosis, in which the cells quickly lose plasma membrane integrity and at later stages release intracellular proteins such as LDH[27]. This strategy is an efficient

mechanism used to clear intracellular bacteria such as *Salmonella* or *Legionella* infections[30]. Here we found that caspase-1 controlled the release of inflammasome particles from macrophages at very early time points after inflammasome activation (10-30 min after activation with ATP or nigericin), with a non-significant increase in extracellular LDH, but with elevated membrane permeabilization. Similarly, cell death induced in COS7 cells by ASC overexpression also leads to the presence of stable extracellular ASC specks[31]. LDH (140 kDa, 26.6 nm) is a cytosolic protein routinely used to monitor cell death, and is smaller than inflammasome particles (1-2 μm)[9], suggesting that pyroptosis could preferentially release different cytosolic components. This could be possible through specific compartmentalization of the cytoplasm, and electron microscopy of nigericin-treated macrophages revealed a compartmentalization of the cytosol, with approximately half of the cytoplasm well structured (with visible organelles and intact plasma membrane), and the rest of the cytoplasm vacuolized and destructured with numerous autophagy vesicles. Autophagy has been recently proposed as a mechanism to limit inflammasome activation[32,33], but also as a novel mechanism for the unconventional release of IL-1β upon caspase-1 activation[34]. The inflammasome speck was found in between, or close to the edge of the cell in the destructured part of the cytoplasm where plasma membrane integrity was compromised. These data suggest that the initial fast release of inflammasome particles could be a result of a polarized cytoplasm in the macrophage during the early events of pyroptosis. Thus while some of the protein pool (i.e. β-actin or LDH) could remain intracellular in the normal side of the cytoplasm, the inflammasome particle and probably also IL-1β are released through a focal side of the cell. We found that a small pool of NLRP3 protein is also released at short time points after inflammasome stimulation (likely as a core component of particulate inflammasome release). This

was followed by a delayed release of the rest of the soluble NLRP3 and this fits with the kinetic release of LDH and β-actin, suggesting that the majority of NLRP3 could be leaking from the cell after the inflammasome particle is released.

The immune system uses different extracellular strategies for the clearance of infectious agents and for the recovery of homeostasis, that for example includes the formation of extracellular nets or circulating immune-complexes[35,36]. It has been recently shown that extracellular neutrophil nets activate caspase-1 via the NLRP3-inflammasome in macrophages[37], and here we describe that the multiprotein inflammasome complex acts as an extracellular danger particle to amplify the inflammatory response through the activation of caspase-1 in neighboring macrophages. Released caspase-1 following inflammasome activation was active and could process pro-IL-1β in the extracellular milieu, expanding the function of caspase-1 to extracellular substrates.

The NLRP3 inflammasome has been classically described as an oligomer consisting of the core sensor protein NLRP3 with the protein ASC being the adapter to recruit pro-caspase-1[2]. Caspase-1 activation then appears to involve auto-cleavage at residues D119, D297 and D316, releasing the large (p20) and small (p10) subunits from the N-terminal CARD domain[38]. In addition, upon NLRP3-inflammasome activation, the majority of ASC protein in the cell oligomerizes into a large complex that was initially linked to pyroptosis and termed the pyroptosome[39]. Recent ultrastructural studies have demonstrated that, upon stimulation, the NLRP3 proteins oligomerize and recruit ASC into fiber-like structures that formed large particles[8,9], therefore unifying the concepts of NLRP3 inflammasome and ASC speck. Our recombinant ASC oligomeric particles also appeared as fiber-like structures that were able to recruit new subunits of ASC and were able to activate caspase-1 in the

extracellular environment. These particles were also internalized by macrophages and induced activation of caspase-1 and release of IL-1β independently of endogenous NLRP3 or ASC. Different to other protein aggregates that activate the NLRP3 inflammasome via lysosomal destabilization, such as β-amyloid or islet amyloid polypeptide[12,40], ASC oligomers were able to induce caspase-1 activation by directly aggregating pro-caspase-1 in macrophages independently of NLRP3.

We also found extracellular inflammasome particles in the serum of patients with active CAPS. Oligomeric NLRP3 particles with mutated gain-of-function subunits were internalized by macrophages, and were able to induce ASC aggregation, caspase-1 activation and IL-1β release in NLRP3-deficient macrophages. It has been reported that both germline and somatic *NLRP3* mutations cause different clinical CAPS phenotypes[41,42]. How low-level somatic *NLRP3* mosaicism causes CAPS is poorly studied. Our data provide new insights into the pathophysiological mechanisms underlying CAPS and somatic *NLRP3* mosaicism, since released inflammasome oligomers containing mutated NLRP3 proteins could activate caspase-1 in monocytes and macrophages carrying exclusively wild-type *NLRP3* alleles. In fact, we found elevated ASC-positive particles in the serum of CAPS patients with low-level somatic *NLRP3* mosaicism. IL-1β is the main driver of the pathophysiology of CAPS, since the different strategies to block IL-1β (anakinra, canakinumab, rilonacept) quickly and completely resolve the clinical and biochemical disease features[43,44,45]. However, serum concentrations of IL-1β are not a good disease biomarker for patients with CAPS, and its diagnosis depends on *NLRP3* genotyping. It was surprising to find no statistical differences on the number of NLRP3 particles in the serum of CAPS patients during disease flare compared with healthy individuals. The ASC/NLRP3 ratio of inflammasome oligomeric particles is extremely high[9] and

that could explain the difficulty in detecting NLRP3 in the serum particles of CAPS patients compared to the detection of ASC-positive particles. Furthermore, the NLRP3 antibody used here was raised against Nt-PYD domain of NLRP3, the domain that interacts with ASC and that could be hardly accessible to the antibody upon activation. This is supported by our previous work, where we have found that the immunoprecipitation efficacy of NLRP3, using a tag located on the N-terminus of the protein, decreases upon stimulation[11], and therefore it could also affect NLRP3 detection in the ASC-positive particles of the serum of CAPS patients. Here we describe that during active disease, patients with CAPS presented increased serum concentrations of ASC-positive particles. This was not observed in the serum of patients with the inherited autoinflammatory diseases FMF and TRAPS, suggesting that ASC determination could represent a novel strategy for diagnosis and follow-up of CAPS. In support of this idea, it has been recently reported that the detection of ASC in cerebrospinal fluid of brain-injured patients correlated with the patients' functional outcome[46].

Taken together, our data demonstrate that inflammasome activation results in the release of active inflammasome oligomers as particles that act extracellularly as danger signals amplifying the inflammatory response by activating caspase-1.

## ACKNOWLEDGEMENTS

We thank E. Latz for ASC and NLRP3 deficient mouse bone marrow immortalized macrophages and for ASC-RFP expression vector; V. Dixit (Genentech) for *Pycard*$^{-/-}$ mice; M.C. Baños and J.J. Martínez for both molecular and cellular technical assistance; L. Martinez-Alarcón for healthy donors blood extraction; M. Martínez-Villanueva for CRP determination; and C. de Torre for support with proteomics. V. Compan was supported by grant from Wellcome Trust. F. Martín-Sánchez and J. Amores-Iniesta were supported by *Sara Borrell* post-doctoral grant from Instituto Salud Carlos III (CD12/00523 and CD13/00059). This work was supported by grants from Instituto Salud Carlos III-FEDER (EMER07/049 to P.P., PS09/00120 to P.P., PS09/01182 to J.Y. and PI13/00174 to P.P.), Fundación Séneca (11922/PI/09 to P.P.) and Fundación Mutua Madrileña (ID98FMM013 to A.B-M.).

## AUTHOR CONTRIBUTIONS

Execution of experiments: A.B-M., F.M-S., C.M.M., J.A-I, V.C., A.I.G., M.B-C.

Human samples and knock-out supply: J.Y., E.R-O., J.A., S.B., J.I.A., I.C.

Analysis and interpretation of data: A.B-M., F.M-S., V.C., A.I.G., J.I.A., D.B., P.P.

Manuscript preparation: A.B-M., F.M-S., V.C., D.B., J.I.A., P.P.

## COMPETING FINANCIAL INTERESTS

The authors declare no competing financial interests.

## FIGURE LEGENDS

**Figure 1** Inflammasome activation induces NLRP3 and ASC release. (**a**) Immunoblot analysis of cell lysate (Lys) and supernatant (Sup) demonstrating the release of inflammasome components in LPS-primed (1 μg/ml, 4h) mouse BMDM after NLRP3 stimulation with nigericin (20 μM) or ATP (5 mM) for 30 min. (**b**) Immunoblot analysis of supernatants to study the time-course for inflammasome component release from macrophages stimulated as in (**a**) for the indicated times. (**c**) Densitometry of released proteins of panels shown in (**b**) normalized to the release at 2h after ATP or nigericin stimulation. (**d**) Percentage of extracellular LDH and membrane permeabilization to YoPro-1 of macrophages treated as in (**a,b**). (**e**) Immunoblot analysis of cell lysate (Lys) and supernatant (Sup) for different inflammasome components in LPS-primed mouse bone marrow derived macrophages after NLRP3 stimulation with MSU crystals (200 μg/ml) or *E. coli* (MOI of 20), NLRP1 stimulation with Anthrax Lethal Toxin (LTx, 2.5 μg/ml), NLRC4 stimulation with flagellin (100 ng/ml), or AIM2 stimulation with poly(dA:dT) (dA:dT, 5 μg/ml), all for 16 h. (**f**) Immunoblot analysis of cell lysate (Lys) and supernatant (Sup) from wild-type (WT) or knock-out mouse BMDMs activated as in (**a**) incubated where indicated with a caspase-1 inhibitor (Ac-YVAD, 50 μM). Immunoblots are representative of at least three independent experiments (**a,e,f**) or two independent experiments (**b**); and histograms in (**d**) are presented as mean ± SEM of three to five independent experiments. *$p < 0.05$; **$p < 0.01$; ***$p < 0.001$; NS, not significant ($p>0.05$) difference compared with control conditions.

**Figure 2** Extracellular inflammasomes are oligomeric particulate complexes. (**a**) Immunoblot of cross-linked (SDA) ASC oligomers reduced or not with β-mercaptoethanol (β-ME) from cell supernatants of LPS-primed (1 μg/ml, 4h) mouse BMDMs after NLRP3 stimulation with nigericin (20 μM, 10 or 30 min), or ATP (5 mM, 30 min). (**b**) Co-immunoprecipitation of ASC and NLRP3 in cell supernatants of LPS-primed BMDMs after NLRP3 stimulation with ATP as described in panel (**a**). (**c,d**) Representative images of BMDMs stimulated as in (**a**), stained for ASC (green), actin (red, phalloidin), membrane (cyan, CTB, in **c**) and nuclei (blue, DAPI) demonstrate that ASC particulate specks could be found outside the cells (arrowhead); ASC specks close to the edge of the cells are denoted by arrows and intracellular ASC specks are denoted by asterisks; bar, 10 μm. (**e**) Quantification of the percentage of ASC specks with respect to the total number of ASC specks present intracellular (In), close to the macrophage edge (Surface), and extracellularly (Out) after NLRP3 stimulation with ATP as indicated in (**a**) for the indicated times. (**f,g**) Detection of ASC and NLRP3 extracellular particles by flow cytometry in cell supernatants of macrophages stimulated as in (**a**) derived from wild-type (WT) (**f,g**), or different knock-out mice as indicated (**g**). Black line histograms in (**f**) correspond to cell-free supernatants of ATP treated macrophages and grey histograms correspond to cell-free supernatants of resting (non ATP treated) macrophages. In panel (**g**) the percentage positive ASC or NLRP3 specks in cell supernatants is represented with respect to the total number of particles gated for small particles. Immunoblots in (**a,b**) are representative of three different experiments. Data are presented as mean ± SEM from $n$ = 3-5 independent experiments for (**g**); and as mean of $n$ = 2-4 independent experiments for (**c**) quantifying >140 cells/experiment from >10 different fields of view/experiment. *$p < 0.01$; **$p < 0.005$; ***$p < 0.001$; NS, not significant ($p>0.05$)

difference compared with control conditions in (**g**) and comparing 20 min with the groups of 5 and 10 min in (**e**).

**Figure 3** ASC specks activate extracellular caspase-1. (**a**) Caspase-1 activity measured in supernatants of LPS-primed (1 μg/ml, 4h) BMDMs derived from wild-type (WT) or knock-out mice as indicated after NLRP3 stimulation with nigericin (20 μM) or ATP (5 mM) for 30 min. (**b**) Immunoblot analysis of the processing of WT or double mutated D27A, D116A pro-IL-1β in presence of recombinant caspase-1 (rec Casp1, 10U) or macrophage cell-free supernatants after NLRP3 stimulation as indicated in (**a**) and incubated where indicated with a caspase-1 inhibitor (Ac-YVAD, 50 μM). (**c**) Caspase-1 activity measured in supernatants of WT or *Nlrp3*$^{-/-}$ BMDMs activated with nigericin (10 μM, 30 min) and then incubated at 37ºC without cells for the indicated times before measuring caspase-1 activity. r = 0.948; p = 0.0003. (**d**) Fluorescence and bright field microscopy of recombinant ASC-YFP specks, bar 0.5 μm. (**e**) Transmission electron microscopy of recombinant ASC-YFP oligomeric specks revealed fiber-like structures, bar 200 nm. (**f**) Transmission electron microscopy of macrophages treated as in (**a**) shows that endogenous ASC specks present a fiber-like structure (asterisk), bar 1 μm. (**g**) Fluorescence microscopy of recombinant ASC-YFP specks nucleating soluble ASC-mCherry, bar 1 μm. (**h,i**) Caspase-1 activity measured in supernatants of WT or *Nlrp3*$^{-/-}$ BMDMs activated with different doses of nigericin as indicated for 30 min. Supernatants were mixed with 5x10$^5$ recombinant ASC-YFP particles for 2 h (in red), alone or in the presence of ATP (5 mM), apyrase (3 U/ml) or 150 mM KCl (High $K^+$) as indicated in (**i**). (**j**) ELISA of released IL-1β from wild-type (WT), *Nlrp3*$^{-/-}$ or *Pycard*$^{-/-}$ LPS-primed immortalized mouse BMDM after NLRP3 stimulation for 30 min with ATP (5 mM),

recombinant ASC-YFP specks (ratio 1:1) or HEK lysates as indicated. Immunoblot in (**b**) is representative of 3-4 independent experiments. Data are presented as mean ± SEM from *n* = 3-9 independent experiments for the different treatments in (**a,c,i,j**). *p < 0.05; **p < 0.005; ***p < 0.001; NS, not significant (p>0.05) difference with selected groups as indicated.

**Figure 4** Extracellular ASC specks activate caspase-1 in macrophages. (**a**) Representative maximum intensity projection image of mouse BMDMs incubated for 1h with recombinant purified ASC-YFP specks and stained for actin (red, phalloidin) and nuclei (blue, DAPI) demonstrating that extracellular ASC specks are internalized; bar, 5 μm; arrowhead denotes ASC speck; bottom and right panels are *z*-stacks. (**b**) ELISA of released IL-1β from wild-type (WT), or knock-out BMDMs as indicated primed with LPS (1 μg/ml, 4h) and activated with ATP (5 mM, 30 min) or recombinant ASC-YFP specks (at 1:1, 1:5 or 1:10 ratio, 3h). (**c**) Caspase-1 activity measured in supernatants from macrophages treated as in (**b**). (**d**) ELISA of released IL-1β from WT BMDMs treated with mock HEK293 purified cell lysate as a negative control or treated as in (**b**) and incubated as indicated with N-acetyl-cysteine (NAC, 10 mM), high extracellular $K^+$ solution (high $K^+$), cytochalasin B (30 μM) or the cathepsin B inhibitor Ca074Me (50 μM). (**e**) Representative images of WT BMDMs treated as in (**b**) and stained for caspase-1 (red) and nuclei (blue, DAPI); bar 5 μm; arrowhead denotes aggregation of caspase-1. (**f**) Number of peritoneal $Gr1^+Mac1^+$ cells in WT or *Casp1*$^{-/-}$*Casp11*$^{-/-}$ mice as indicated after intraperitoneal injection of vehicle or $4x10^6$ of purified recombinant ASC-YFP specks for 16 h. (**g**) ELISA of IL-1β from peritoneal lavage of WT animals treated as in (**f**). Data are presented as mean ± SEM from *n* = 3 independent experiments. Dots in (**f,g**) represent independent

animals from three different experiments. *p < 0.05; **p < 0.005; ***p < 0.001; NS, not significant (p>0.05) difference with selected groups as indicated or with control condition in (**c**).

**Figure 5** p.D303N *NLRP3* mutant forms functional oligomeric specks that nucleate ASC. (**a**) Representative images of HEK293 cells expressing wild-type (WT) or different NLRP3-YFP mutants associated to CAPS as indicated and stained for actin (red, phalloidin) and nuclei (blue, DAPI). NLRP3 mutants, but not WT, aggregate in specks; bar, 10 μm. (**b**) Representative images of HEK293 cells expressing the $P_2X_7$ receptor and the p.D303N NLRP3-YFP mutant and stained as in (**a**) after treatment with ATP (3 mM, 30 min) as indicated. p.D303N NLRP3-YFP particles are released from cells (arrowheads) upon ATP stimulation; bar, 10 μm. (**c,d**) Detection of extracellular p.D303N NLRP3-YFP particles by flow cytometry (**c**) or immunoblot (**d**) in cell supernatants of cells treated as in (**b**). The black line in the histogram in (**c**) corresponds to supernatants of ATP treated cells and the grey histogram corresponds to supernatants of resting (non ATP treated) cells. (**e**) Percentage of LDH in supernatants respect to total intracellular LDH (left) and percentage of cells permeable to YoPro-1 with respect to the total number of cells (right) from cells treated as in (**b**). (**f**) Fluorescence and bright field microscopy of recombinant p.D303N NLRP3-YFP particles, bar 5 μm. (**g**) Transmission electron microscopy of recombinant p.D303N NLRP3-YFP particles demonstrates globular-like structures, bar 50 nm. (**h**) Representative images of HEK293 cells expressing p.D303N NLRP3-YFP mutant and ASC-RFP and stained for nuclei (blue, DAPI). Note that the NLRP3 mutant appears adjacent to ASC oligomers (arrows); bar, 5 μm. (**i**) Flow cytometry of supernatants from LPS-primed (1 μg/ml, 4h) WT or *Pycard*$^{-/-}$ mouse BMDMs treated

or not with ATP (5 mM, 30 min) as indicated. Then cell-free supernatants were mixed with $5x10^5$ p.D303N NLRP3-YFP particles and stained for ASC. p.D303N NLRP3-YFP particles were able to nucleate ASC in the absence of macrophages and appears as a double positive particle population. (**j**) Representative images of recombinant p.D303N NLRP3-YFP particles nucleating soluble ASC-mCherry (arrows), bar 2 μm. Immunoblot in (**d**), histograms in (**c**) and plots in (**i**) are representative of two different experiments. Data are presented as mean ± SEM from $n = 4$ independent experiments for (**e**); **p < 0.005; ***p < 0.001 with respect to the control group.

**Figure 6** Extracellular p.D303N NLRP3 particles form functional inflammasomes in macrophages upon internalization. (**a,b**) ELISA of released IL-1β from LPS-primed wild-type (WT) (**a**) or different knock-out mouse BMDMs as indicated in (**b**) after incubation with p.D303N NLRP3-YFP particles at 1:1 ratio for different times as indicated in (**a**) or for 16h in (**b**). (**c**) Caspase-1 activity measured in supernatants from WT macrophages treated as in (**b**). (**d**) Representative fluorescence microscopy images from WT macrophages treated as in (**b**) for 30 min and immunostained for ASC (red) and nuclei (blue, DAPI), demonstrate upon p.D303N NLRP3-YFP particle ingestion intracellular ASC aggregates into a speck (arrowhead); bar, 10 μm. (**e**) Quantification of the number of WT or *Nlrp3*$^{-/-}$ BMDMs with intracellular ASC speck treated as in (**d**). (**f**) Detection of ASC particles in WT macrophage supernatants by flow cytometry of WT macrophages treated as in (**b**) for 3 h (black line on histogram); grey histogram corresponds to supernatants of untreated macrophages. (**g,h**) ELISA of released IL-1β (**g,h**) and phagocytosis of p.D303N NLRP3-YFP particles (**g**) from LPS-primed WT mouse BMDMs after stimulation with p.D303N NLRP3-YFP particles for 16 h treated or not with cytochalasin B (20

μM) (**g**) or with N-acetyl-cysteine (NAC, 10 mM), high extracellular $K^+$ solution (High $K^+$) or the cathepsin B inhibitor Ca074Me (50 μM) (**h**). (**i**) Number of peritoneal $Gr1^+Mac1^+$ cells in WT and *Pycard*$^{-/-}$ mice after intraperitoneal injection of vehicle solution or $4x10^6$ purified recombinant p.D303N NLRP3-YFP particles for 16 h. (**j**) ELISA of IL-1β from peritoneal lavage of animals treated as in (**i**). Histograms in (**f**) are representative of two different experiments. Data are presented as mean ± SEM from $n$ = 3-10 independent experiments for (**a-c,g,h**); and as mean of $n$ = 2 independent experiments for (**e**) quantifying >300 cells/experiment from 4-8 different fields of view/experiment. Dots in (**i,j**) represent independent animals from three different experiments. *p < 0.05; **p < 0.005; ***p < 0.001; NS, not significant (p>0.05) difference among indicated groups.

**Figure 7** Extracellular inflammasome particles are present in the serum of patients with CAPS. (**a**) Representative fluorescence images of human serum immunostained for ASC (green) from a healthy donor and two patients with different active CAPS phenotypes (MWS and CINCA with the corresponding *NLRP3* mutations as indicated). Left panel is a control with sterile PBS instead of serum. Arrowhead denotes ASC aggregates as irregular particles; bar, 50 μm. (**b**) Flow cytometry detection of ASC and NLRP3 particles in the serum of patients with different active CAPS phenotypes (FCAS, MWS and CINCA with the corresponding *NLRP3* mutations as indicated; black line on histograms), compared to healthy donors (gray filled histograms). (**c**) Detection of CRP in the serum of healthy donors and patients with different autoinflammatory syndromes as indicated, including CAPS patients with active symptoms (CRP >10 mg/l), CAPS patients during symptom free interval (CRP <10 mg/l) and CAPS patients with low-grade somatic mosaicism for NLRP3.

(**d,e**) Percentage of ASC (**d**) or NLRP3 (**e**) particles gated for small particles in the serum of the groups represented in (**c**). Background staining was established using the fluorescent secondary antibody alone and median (continuous gray line), and 75 and 25 percentiles (dashed gray lines) for background is shown in the panels (**d,e**). (**f**) Detection of pro-inflammatory IL-1β and IL-6 cytokines in the serum of the groups represented in (c). *$p < 0.05$; **$p < 0.005$; ***$p < 0.001$; NS, not significant ($p>0.05$) difference compared to the healthy group.

## ONLINE METHODS

**Animals.** Wild-type C57BL/6J mice were purchased from Harlan, *Nlrp3*$^{-/-}$ [6], *Pycard*$^{-/-}$ [47] and *Casp1/11*$^{-/-}$ [48] all on C57BL/6J background were maintained in specific pathogen-free conditions at a room temperature of 20 ± 2°C, and a 12 h:12 h light/dark cycle. The mice were fed a sterile commercial pellet diet and sterile tap water ad libitum. The procedure of peritonitis in mice induced by intraperitoneal injection of particles was approved by the "*Servicio de Sanidad Animal, Dirección General de Ganadería y Pesca, Consejería de Agricultura y Agua Región de Murcia*" (Health Animal Service, Murcia Fishing and Farming Council) with reference C1310050308. In brief, mice were used at 6-10 weeks of age and were randomized in groups and intraperitoneally injected with saline vehicle solution or with $4x10^6$ of ASC-YFP or p.D303N NLRP3-YFP recombinant particles for 16 h. Sample size was estimated according to our previous experience and other similar published work[6]. The researchers were not blinded to the groups.

**Human samples.** Whole peripheral blood samples were collected after obtaining written informed consent from healthy donors (n = 8) and from patients with different monogenic inherited autoinflammatory syndromes (twenty eight patients with cryopyrin-associated periodic syndromes, six patients with Familial Mediterranean Fever and six patients with TNF Receptor-associated periodic syndrome), see **Supplementary Table 1**. The serum fraction of these samples was separated by centrifugation at 680 xg for 5 min and frozen at -80ºC. The Institutional Review Board of Hospital Clínic approved the use these serum samples.

**Reagents.** *E. coli* LPS O55:B5, DAPI, ATP, cytochalasin B, triton X-100, N-Acetyl-L-cysteine (NAC) and nigericin (Sigma); Recombinant caspase-1, caspase-1 inhibitor Ac-YVAD-AOM and the specific caspase-1 substrate z-YVAD-AFC were from Merk-Millipore; MSU crystals (Enzo Life Sciences); Flagellin from *S. typhimurium* and poly(dA:dT)/LyoVec were from Invivogen; receptor-binding protein protective antigen (PA) and metalloprotease lethal factor (LF) were from List Biological; the protein delivery reactive PULSin from PolyPlus Transfection; Phalloidin-Rhodamine and Abs for β-actin (clone C4)-HRP (sc-47778HRP), GFP clone FL (sc-8334), caspase-1 p10 rabbit polyclonal clone M-20 (sc-514), IL-1β clone H-153 (sc-7884) and ASC clone (N-15)-R (sc-22514-R) were from Santa Cruz Biotechnology. Mouse monoclonal anti-NLRP3 clone Cryo-2 (AG-20B-0014), mouse monoclonal anti-caspase-1 p20 clone Casper-1 (AG-20B-0042) and rabbit polyclonal anti-ASC clone AL177 (AG-25B-0006) were from AdipoGen. Ca074Me was from Merk-Millipore. All HRP-conjugated secondary Abs were from GE Healthcare and fluorescent-conjugated secondary Abs and cholera toxin B-Alexa Fluor 647 were from Life Technologies.

**Cells and treatments.** Bone marrow derived macrophages (BMDM) were obtained from C57BL/6J or from knock-out mice as previously described[11]. HEK293T cells (ATCC CRL-11268) were maintained DMEM:F12 (1:1) media, supplemented with 10% fetal calf serum (FCS), 2 mM glutamax and 1 % pen/strep (Life Technologies) and routinely tested for mycoplasma contamination using the (Roche). Lipofectamine 2000 reagent (Life Technologies) was used to transfect HEK293 cells under manufacturer's instructions. For stable HEK293 cell selection, the different mutations of NLRP3-YFP were generated by overlapping PCR and cloned in pcDNA3.1/V5-His

TOPO (Life Technologies). After sequencing for correct mutations, the vectors were transfected as mentioned, and two days later the cell culture media was supplemented with G418 (2 mg/ml, Acros Organic) for 4 weeks. Cell cloning was then performed by serial dilution in 96 well plates in the presence of G418 for further 4-8 weeks and positive clones were expanded. Immortalized mouse BMDMs from wild-type, *Pycard*$^{-/-}$ or *Nlrp3*$^{-/-}$ mice were a generous gift of E. Latz and were maintained as previously described[17]. All macrophages were primed with LPS (1 μg/ml, 4 h) and subsequent NLRP3 activation was achieved with ATP (5 mM, 30 min), nigericin (20 μM, 30 min), MSU crystals (200 μg/ml, 16 h), or live *E. coli* (MOI 20, for 1 h and then addition of 100 U/ml pen/strep and incubate for further 16 h). Activation of NLRP1, NLRC4 or AIM2 inflammasomes was carried out by using Anthrax Lethal Toxin (2.5 μg/ml receptor-binding protein PA and 1 μg/ml metalloprotease LF mix, 16 h), flagelin (100 ng of recombinant protein were mixed with the protein delivery reagent PULSin and cells incubated during 16 h) or poly(dA:dT) (5 μg/ml of poly(dA:dT)/LyoVec, 16 h), respectively. ASC-YFP or NLRP3-D3030N-YFP recombinant particles were incubated at different particle:macrophage ratios as explained in figure legends. After cell stimulation, cell supernatants were collected centrifuged (300 x*g*, 8 min, 4ºC) to eliminate cells detached due to cell death to generate cell-free medium preparations. Before analysis, supernatant proteins (soluble and insoluble) were concentrated by centrifugation (11,200 x*g*, 30 min, 4ºC) through a 10-kDa cut-off column (Microcon® Merk-Millipore). All supernatants were free of genomic DNA as measured by absorbance at 260 nm and PCR amplification and therefore we discarded any dying cell contamination.

**Recombinant ASC and NLRP3 particle isolation.** HEK293 cells transiently expressing ASC-YFP, or stably expressing p.D303N NLRP3-YFP mutant, were used to isolate inflammasome particles as previously described[49]. Briefly, cells were lysed in buffer A (20 mM HEPES-KOH, pH 7.5, 10 mM KCl, 1.5 mM $MgCl_2$, 1 mM EDTA, 1 mM EGTA, 320 mM sucrose) by passing the lysate 30 times through a 1 ml syringe with a 25-gauge needle at 4ºC. The cell lysate was centrifuged (400 x*g*, 8 min) and the supernatant was filtered using a 5 μm filter (Millipore). The clarified cell lysate was diluted with one volume of CHAPS buffer (20 mM HEPES-KOH, pH 7.5, 5 mM $MgCl_2$, 0.5 mM EGTA, 0.1 mM PMSF, 0.1 % CHAPS) and then centrifuged to pellet ASC or p.D303N NLRP3 oligomeric complex structures, and washed in CHAPS buffer. ASC-YFP and p.D303N NLRP3-YFP were then subjected to percoll gradient and inflammasome particles were separated, washed in CHAPS buffer and quantified by counting the number of fluorescent particles using a Bürker chamber. ASC-YFP and p.D303N NLRP3-YFP particles were then adjusted to $5x10^5$ specks/μl. As control, lysate from mock transfected HEK293 cells were subjected to this protocol and the final product was used as negative control in the experiments.

**Immunocytochemistry and fluorescence microscopy.** Macrophages stimulated on coverslips were washed twice with PBS, incubated for 10 min with cholera toxin B-Alexa Fluor 647 (1:2500 dilution) and fixed with 4% formaldehyde in PBS for 15 min at room temperature, and then washed three times with PBS. Cells were blocked with 1 % bovine serum albumin (Sigma) and permeabilized with 0.2 % saponin (Fluka) in PBS for 30 min at room temperature before incubating with primary antibody. Primary antibodies used were rabbit anti-ASC (1:200, Santa Cruz Biotechnology) or anti-caspase-1 (1:200, Addipogen). Primary antibodies were incubated for 1 h at room

temperature. Cells were washed and incubated with appropriate fluorescence-conjugated secondary antibody (1:200) for 2 h at room temperature, then rinsed in PBS and incubated for 20 min with phalloidin-rhodamine (300 nM). All coverslips were mounted on slides with Fluoroshield with DAPI (Sigma).

Nucleation experiments were performed by incubating soluble ASC-mCherry with $5x10^5$ of ASC-YFP or mutated NLRP3-YFP particles for 2h at 37ºC in CHAPS buffer. To produce soluble ASC-mCherry, unstimulated ASC-mCherry immortalized macrophages were lysed in CHAPS buffer by syringing 20 times with a 25-gauge needle at 4ºC. The cell lysate was centrifuged (14000 rpm, 8 min) and the clarified cell lysate was then centrifuged (23,000 x*g*, 1h) to generate a particulate free supernatant.

Images were acquired with a Nikon Eclipse Ti microscope equipped with 20x/0.45 S Plan Fluor, 40x/0.60 S Plan Fluor and 60x/1.40 Plan Apo Vc objectives and a digital Sight DS-QiMc camera (Nikon), a Z optical spacing of 0.2 μm and the 387nm/447nm, 472nm/520nm, 543nm/593nm and 650nm/668nm filter sets (Semrock). Maximum intensity projection of images was achieved using the NIS-Elements AR software (Nikon) amd ImageJ (NHI).

**Electron microscopy.** Recombinant ASC or NLRP3 particles and macrophages stimulated on suspension were centrifuged and pellets were fixed in 2.5% buffered glutaraldehide (Sigma) in 0.1M cacodilatre buffer for 1.5h at 4ºC. After fixation, the pellets were immersed in 0.01M cacodylate buffer solution for 8h, postfixed in 1% osmium tetroxide (Sigma) in 0.1M cacodilate buffer for 2h in the dark, and counterstained with 2% uranyl acetate (Sigma) in Michaelis sodium acetate/sodium veronal buffer for 2h. The pellets were then dehydrated in an increasing ethanol

gradient (30%, 50%, 70%, 90% and 100%), immersed in propylene oxide (Sigma) for 15 min and then in 1:1 propylene oxide/Epon812 resin (Tousimis) for 16h. The solution was then changed for pure Epon812 solution for 3h. The pellets were then located in capsules, embedded in fresh Epon812 and incubated for 72h at 70ºC. Ultrathin sections (40 nm) were obtained from specimens using a microtome (Leyca microsystems) and placed onto copper grids (Sigma). Grids were finally post-stained by immersing them in 2% uranyl acetate in veronal buffer (Lonza) for 2h, and in lead citrate (SPI) for 5 min. Grids were then visualized in a Jeol JEM-1011 transmission electron microscope.

**Flow cytometry.** For the detection of extracellular ASC and NLRP3 particles 0.5 ml of human serum or culture cell supernatants from stimulated macrophages were incubated with 1 μg of rabbit polyclonal anti-ASC (Adipogen) and mouse monoclonal anti-NLRP3 (Adipogen) for 1h. Particles were centrifuged and washed before incubation with secondary antibodies anti-rabbit IgG Alexa Fluor 647 and anti-mouse IgG R-PE (Life Technologies). Samples were washed before being subjected to flow cytometry analysis using a BD FACSCanto flow cytometer with the FACSDiva software (BD Biosciences) by gating for small particles or cell debris based on FSC versus SSC parameters which were adjusted to display a correct separation of leukocyte populations. Gated events were displayed on a histogram plot where the percentage of positive particles was determined.

Peritoneal cells from mice injected with saline vehicle solution, ASC-YFP or NLRP3-YFP particles were counted, washed and incubated with Mouse SeroBlock FcR (ABD Serotec) for 10 min. The cells were then incubated with anti-mouse GR1 R-PE conjugated antibody (BD Biosciences) and anti-mouse CD11b (Mac-1) APC

conjugated antibody (BD Biosciences) for 30 min. Cells were subjected to flow cytometry analysis by gating leukocytes based on SSC vs FSC parameters.

**Co-immunoprecipitation, ASC oligomerization and immunoblotting.** Detailed methods used for immunoblot analysis and ASC oligomerization cross-linking have been described previously[11,49]. Immunoblot results were analyzed by densitometry measurements using Quantity One software (BioRad). For co-immunoprecipitation, equal amounts of cell supernatant were incubated with 1.5 μg of anti-ASC or irrelevant rabbit IgG (1 h, 4ºC) and then with prot-G-agarose beads (Merk-Millipore, 1 h, 4ºC). Beads were washed 3 times and heated (5 min, 80ºC) with reducing loading sample buffer (Life Technologies). Stable expressing HEK293 cells for pro-IL-1β-YFP construction were lysed in cell lysis buffer (25 mM HEPES pH 7.5, 5 mM $MgCl_2$, 5 mM EDTA, 5 mM DTT) and lysates were incubated for 2h at 37ºC with 10U of recombinant caspase-1 or concentrated supernatants from ATP or nigericin treated macrophages supplemented or not with 50 μM caspase-1 inhibitor (Ac-YVAD-AOM).

**ELISA, multiplex, LDH release, Caspase-1 activity measurements and CRP determination.** IL-1β ELISA kit for either human or mouse IL-1β were from R&D. Simultaneous determination of IL-6, IL-1β and TNF-α in human serum samples was performed by using a Cytometric Bead Array Enhanced Sensitivity 3 Plex Set (BD Biosciences) following the manufacturer's instructions. CRP in serum was measured by immuno-turbidimetric method using a Cobas 6000 with c501 module (Roche Diagnostics). Extracellular LDH was detected using the Cytotoxicity Detection kit (Roche) and expressed as the percent of total intracellular LDH. Caspase-1 activity

was measured monitoring the cleavage of the fluorescent substrate z-YVAD-AFC at 400/505 using a Synergy Mx plate reader (BioTek) during 30 min intervals for 6h. Results are presented as either the relative fluorescence units (RFU) or caspase-1 units calculated using a standard curve generated with different concentrations of recombinant caspase-1.

**Membrane permeabilization.** Dye uptake experiments were carried out using a Synergy Mx plate reader (BioTek), and YoPro-1 (Life Technologies) bound to DNA fluorescence was measured at 485/515 nm excitation/emission. The cells were preincubated with 2.5 μM YoPro-1. The fluorescence signal was recorded at 6 s intervals for 30 min before and during incubation at 37 °C with ATP (5 mM) or nigericin (20 μM). Maximum fluorescence was obtained by permeabilizing the cells with Triton-X100 (0.1%).

**Statistical analysis.** Statistics were calculated using Prism software (GraphPad). Giving the differences found in cytokine release from primed macrophages in our previous work, the sample size chosen ensured the adequate power to detect pre-specified effect size. The data allow the evaluation of distribution normality by Kolmogorov-Smirnov test (alpha=0.05). For two-group comparisons a two-tailed unpaired *t*-test was used. Comparisons of multiple groups were analyzed using one-way ANOVA with Bonferroni's multiple comparison test or Dunnett's test to compare all groups with the control group. We found that the variance from the groups compared does not present statistically significant differences.

## REFERENCES


1. Dinarello CA. Immunological and inflammatory functions of the interleukin-1 family. *Annu Rev Immunol* 2009, **27:** 519-550.

2. Schroder K, Tschopp J. The inflammasomes. *Cell* 2010, **140**(6)**:** 821-832.

3. Lopez-Castejon G, Brough D. Understanding the mechanism of IL-1β secretion. *Cytokine Growth Factor Rev* 2011, **22**(4)**:** 189-195.

4. Dinarello CA, Donath MY, Mandrup-Poulsen T. Role of IL-1beta in type 2 diabetes. *Curr Opin Endocrinol Diabetes Obes* 2010, **17**(4)**:** 314-321.

5. Neven B, Callebaut I, Prieur A-M, Feldmann J, Bodemer C, Lepore L*, et al.* Molecular basis of the spectral expression of CIAS1 mutations associated with phagocytic cell-mediated autoinflammatory disorders CINCA/NOMID, MWS, and FCU. *Blood* 2004, **103**(7)**:** 2809-2815.

6. Martinon F, Pétrilli V, Mayor A, Tardivel A, Tschopp J. Gout-associated uric acid crystals activate the NALP3 inflammasome. *Nature* 2006, **440**(7081)**:** 237-241.

7. Duewell P, Kono H, Rayner KJ, Sirois CM, Vladimer G, Bauernfeind FG*, et al.* NLRP3 inflammasomes are required for atherogenesis and activated by cholesterol crystals. *Nature* 2010, **464**(7293)**:** 1357-1361.

8. Cai X, Chen J, Xu H, Liu S, Jiang QX, Halfmann R*, et al.* Prion-like Polymerization Underlies Signal Transduction in Antiviral Immune Defense and Inflammasome Activation. *Cell* 2014, **156**(6)**:** 1207-1222.

9. Lu A, Magupalli VG, Ruan J, Yin Q, Atianand MK, Vos MR*, et al.* Unified Polymerization Mechanism for the Assembly of ASC-Dependent Inflammasomes. *Cell* 2014, **156**(6)**:** 1193-1206.

10. Mariathasan S, Weiss DS, Newton K, McBride J, O'Rourke K, Roose-Girma M*, et al.* Cryopyrin activates the inflammasome in response to toxins and ATP. *Nature* 2006, **440**(7081)**:** 228-232.

11. Compan V, Baroja-Mazo A, López-Castejón G, Gómez A, Martínez C, Angosto D*, et al.* Cell volume regulation modulates NLRP3 inflammasome activation. *Immunity* 2012, **37:** 487-500.

12. Halle A, Hornung V, Petzold GC, Stewart CR, Monks BG, Reinheckel T*, et al.* The NALP3 inflammasome is involved in the innate immune response to amyloid-beta. *Nat Immunol* 2008, **9**(8)**:** 857-865.

13. Babelova A, Moreth K, Tsalastra-Greul W, Zeng-Brouwers J, Eickelberg O, Young MF*, et al.* Biglycan, a danger signal that activates the NLRP3 inflammasome via toll-like and P2X receptors. *J Biol Chem* 2009, **284**(36)**:** 24035-24048.

14. Yazdi AS, Guarda G, Riteau N, Drexler SK, Tardivel A, Couillin I*, et al.* Nanoparticles activate the NLR pyrin domain containing 3 (Nlrp3) inflammasome and cause pulmonary inflammation through release of IL-1α and IL-1β. *Proc Natl Acad Sci USA* 2010, **107**(45)**:** 19449-19454.

15. Eisenbarth SC, Colegio OR, O'Connor W, Sutterwala FS, Flavell RA. Crucial role for the Nalp3 inflammasome in the immunostimulatory properties of aluminium adjuvants. *Nature* 2008, **453**(7198)**:** 1122-1126.

16. Rajamaki K, Nordstrom T, Nurmi K, Akerman KE, Kovanen PT, Oorni K*, et al.* Extracellular acidosis is a novel danger signal alerting innate immunity via the NLRP3 inflammasome. *J Biol Chem* 2013, **288**(19)**:** 13410-13419.

17. Hornung V, Bauernfeind F, Halle A, Samstad EO, Kono H, Rock KL*, et al.* Silica crystals and aluminum salts activate the NALP3 inflammasome through phagosomal destabilization. *Nat Immunol* 2008, **9**(8)**:** 847-856.

18. Lopez-Castejon G, Luheshi NM, Compan V, High S, Whitehead RC, Flitsch S*, et al.* Deubiquitinases regulate the activity of caspase-1 and interleukin-1beta secretion via assembly of the inflammasome. *J Biol Chem* 2013, **288**(4)**:** 2721-2733.

19. Shimada K, Crother TR, Karlin J, Dagvadorj J, Chiba N, Chen S*, et al.* Oxidized mitochondrial DNA activates the NLRP3 inflammasome during apoptosis. *Immunity* 2012, **36**(3)**:** 401-414.

20. Zhou R, Tardivel A, Thorens B, Choi I, Tschopp J. Thioredoxin-interacting protein links oxidative stress to inflammasome activation. *Nat Immunol* 2009.

21. Munoz-Planillo R, Kuffa P, Martinez-Colon G, Smith BL, Rajendiran TM, Nunez G. K(+) Efflux Is the Common Trigger of NLRP3 Inflammasome Activation by Bacterial Toxins and Particulate Matter. *Immunity* 2013, **38**(6)**:** 1142-1153.

22. Murakami T, Ockinger J, Yu J, Byles V, McColl A, Hofer AM*, et al.* Critical role for calcium mobilization in activation of the NLRP3 inflammasome. *Proc Natl Acad Sci U S A* 2012, **109**(28)**:** 11282-11287.

23. Lamkanfi M, Sarkar A, Vande Walle L, Vitari AC, Amer AO, Wewers MD*, et al.* Inflammasome-Dependent Release of the Alarmin HMGB1 in Endotoxemia. *J Immunol* 2010, **185**(7)**:** 4385-4392.

24. Keller M, Rüegg A, Werner S, Beer H-D. Active caspase-1 is a regulator of unconventional protein secretion. *Cell* 2008, **132**(5)**:** 818-831.

25. Pétrilli V, Papin S, Dostert C, Mayor A, Martinon F, Tschopp J. Activation of the NALP3 inflammasome is triggered by low intracellular potassium concentration. *Cell Death Differ* 2007, **14**(9)**:** 1583-1589.

26. Kahlenberg JM, Lundberg KC, Kertesy SB, Qu Y, Dubyak GR. Potentiation of caspase-1 activation by the P2X7 receptor is dependent on TLR signals and

requires NF-kappaB-driven protein synthesis. *J Immunol* 2005, **175**(11)**:** 7611-7622.

27. Miao EA, Rajan JV, Aderem A. Caspase-1-induced pyroptotic cell death. *Immunol Rev* 2011, **243**(1)**:** 206-214.

28. Masters SL, Simon A, Aksentijevich I, Kastner DL. Horror autoinflammaticus: the molecular pathophysiology of autoinflammatory disease. *Annu Rev Immunol* 2009, **27:** 621-668.

29. Gross O, Yazdi AS, Thomas CJ, Masin M, Heinz LX, Guarda G*, et al.* Inflammasome activators induce interleukin-1alpha secretion via distinct pathways with differential requirement for the protease function of caspase-1. *Immunity* 2012, **36**(3)**:** 388-400.

30. Miao EA, Leaf IA, Treuting PM, Mao DP, Dors M, Sarkar A*, et al.* Caspase-1-induced pyroptosis is an innate immune effector mechanism against intracellular bacteria. *Nat Immunol* 2010, **11**(12)**:** 1136-1142.

31. Balci-Peynircioglu B, Waite AL, Schaner P, Taskiran ZE, Richards N, Orhan D*, et al.* Expression of ASC in renal tissues of familial mediterranean fever patients with amyloidosis: postulating a role for ASC in AA type amyloid deposition. *Exp Biol Med (Maywood)* 2008, **233**(11)**:** 1324-1333.

32. Shi CS, Shenderov K, Huang NN, Kabat J, Abu-Asab M, Fitzgerald KA*, et al.* Activation of autophagy by inflammatory signals limits IL-1beta production by targeting ubiquitinated inflammasomes for destruction. *Nat Immunol* 2012, **13**(3)**:** 255-263.

33. Nakahira K, Haspel JA, Rathinam VA, Lee SJ, Dolinay T, Lam HC*, et al.* Autophagy proteins regulate innate immune responses by inhibiting the release of mitochondrial DNA mediated by the NALP3 inflammasome. *Nat Immunol* 2011, **12**(3)**:** 222-230.

34. Dupont N, Jiang S, Pilli M, Ornatowski W, Bhattacharya D, Deretic V. Autophagy-based unconventional secretory pathway for extracellular delivery of IL-1β. *EMBO J* 2011, **30**(23)**:** 4701-4711.

35. Brinkmann V, Reichard U, Goosmann C, Fauler B, Uhlemann Y, Weiss DS*, et al.* Neutrophil extracellular traps kill bacteria. *Science* 2004, **303**(5663)**:** 1532-1535.

36. Shmagel KV, Chereshnev VA. Molecular bases of immune complex pathology. *Biochemistry (Mosc)* 2009, **74**(5)**:** 469-479.

37. Kahlenberg JM, Carmona-Rivera C, Smith CK, Kaplan MJ. Neutrophil extracellular trap-associated protein activation of the NLRP3 inflammasome is enhanced in lupus macrophages. *J Immunol* 2013, **190**(3)**:** 1217-1226.

38. Garcia-Calvo M, Peterson EP, Rasper DM, Vaillancourt JP, Zamboni R, Nicholson DW*, et al.* Purification and catalytic properties of human caspase family members. *Cell Death Differ* 1999, **6**(4)**:** 362-369.

39. Fernandes-Alnemri T, Wu J, Yu J-W, Datta P, Miller B, Jankowski W*, et al.* The pyroptosome: a supramolecular assembly of ASC dimers mediating inflammatory cell death via caspase-1 activation. *Cell Death Differ* 2007, **14**(9)**:** 1590-1604.

40. Masters SL, Dunne A, Subramanian SL, Hull RL, Tannahill GM, Sharp FA*, et al.* Activation of the NLRP3 inflammasome by islet amyloid polypeptide provides a mechanism for enhanced IL-1beta in type 2 diabetes. *Nat Immunol* 2010, **11**(10)**:** 897-904.

41. Tanaka N, Izawa K, Saito MK, Sakuma M, Oshima K, Ohara O*, et al.* High incidence of NLRP3 somatic mosaicism in patients with chronic infantile neurologic, cutaneous, articular syndrome: results of an International Multicenter Collaborative Study. *Arthritis Rheum* 2011, **63**(11)**:** 3625-3632.

42. Nakagawa K, Gonzalez- Roca E, Souto A, Kawai T, Umebayashi H, Campistol J*, et al.* Somatic NLRP3 mosaicism in Muckle-Wells syndrome. A genetic mechanism shared by different phenotypes of cryopyrin-associated periodic syndromes. *Ann Rheum Dis* 2014(doi: 10.1136/annrheumdis-2013-204361).

43. Hoffman HM, Rosengren S, Boyle DL, Cho JY, Nayar J, Mueller JL*, et al.* Prevention of cold-associated acute inflammation in familial cold autoinflammatory syndrome by interleukin-1 receptor antagonist. *Lancet* 2004, **364**(9447)**:** 1779-1785.

44. Hoffman HM, Throne ML, Amar NJ, Sebai M, Kivitz AJ, Kavanaugh A*, et al.* Efficacy and safety of rilonacept (interleukin-1 Trap) in patients with cryopyrin-associated periodic syndromes: results from two sequential placebo-controlled studies. *Arthritis Rheum* 2008, **58**(8)**:** 2443-2452.

45. Lachmann HJ, Kone-Paut I, Kuemmerle-Deschner JB, Leslie KS, Hachulla E, Quartier P*, et al.* Use of canakinumab in the cryopyrin-associated periodic syndrome. *N Engl J Med* 2009, **360**(23)**:** 2416-2425.

46. Adamczak S, Dale G, de Rivero Vaccari JP, Bullock MR, Dietrich WD, Keane RW. Inflammasome proteins in cerebrospinal fluid of brain-injured patients as biomarkers of functional outcome: clinical article. *J Neurosurg* 2012, **117**(6)**:** 1119-1125.

47. Mariathasan S, Newton K, Monack DM, Vucic D, French DM, Lee WP*, et al.* Differential activation of the inflammasome by caspase-1 adaptors ASC and Ipaf. *Nature* 2004, **430**(6996)**:** 213-218.

48. Kuida K, Lippke JA, Ku G, Harding MW, Livingston DJ, Su MS*, et al.* Altered cytokine export and apoptosis in mice deficient in interleukin-1 beta converting enzyme. *Science* 1995, **267**(5206)**:** 2000-2003.

49. Fernandes-Alnemri T, Alnemri ES. Assembly, purification, and assay of the activity of the ASC pyroptosome. *Meth Enzymol* 2008, **442:** 251-270.

# Figure 1

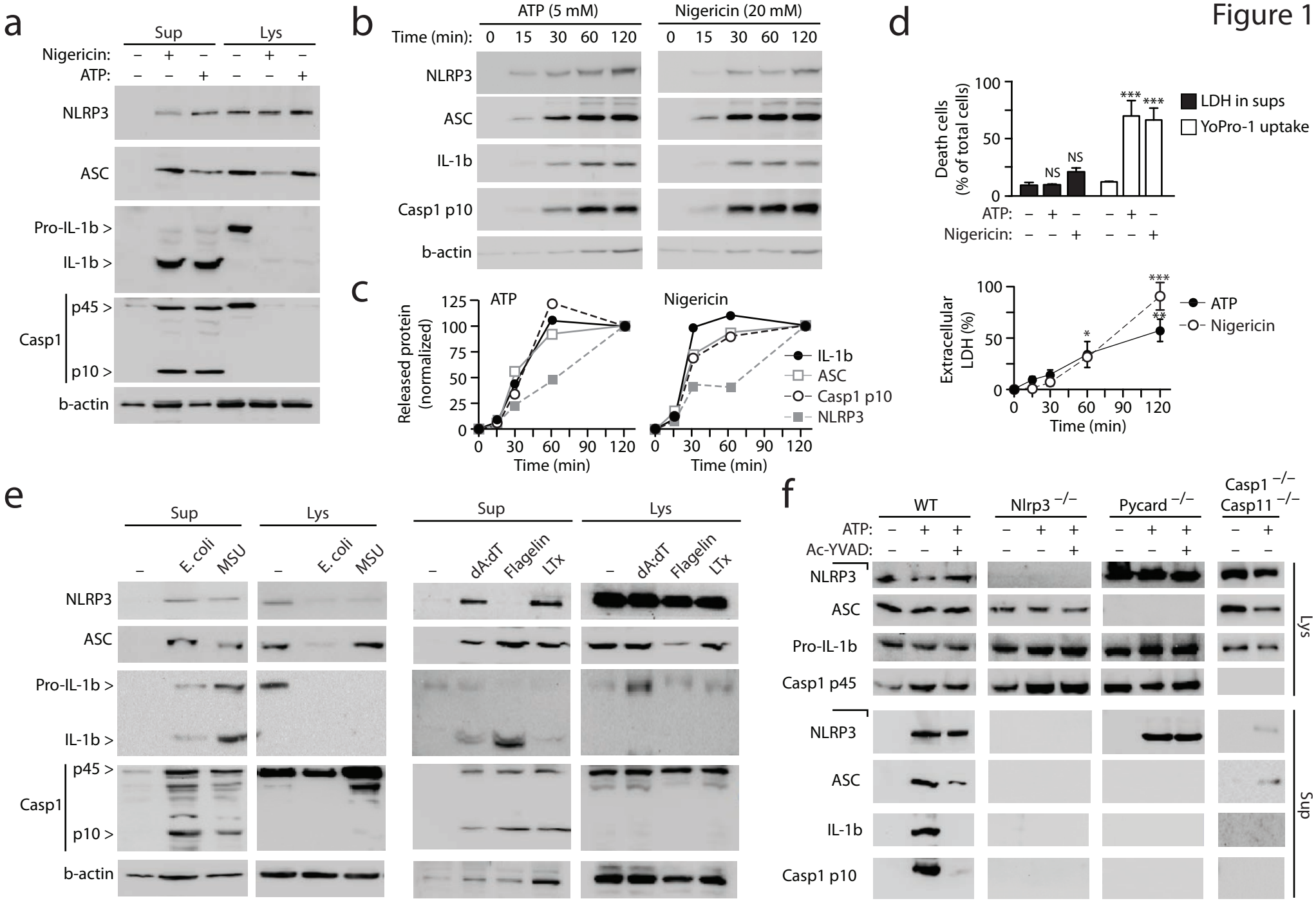
a
Sup
Lys
Nigericin:
ATP:
NLRP3
ASC
Pro-IL-1b >
IL-1b >
Casp1
p45 >
p10 >
b-actin
b
ATP (5 mM)
Nigericin (20 mM)
Time (min): 0 15 30 60 120
NLRP3
ASC
IL-1b
Casp1 p10
b-actin
c
ATP
Nigericin
Released protein (normalized)
Time (min)
IL-1b
ASC
Casp1 p10
NLRP3
d
Death cells (% of total cells)
LDH in sups
YoPro-1 uptake
NS
***
ATP:
Nigericin:
Extracellular LDH (%)
Time (min)
e
Sup
Lys
E. coli
MSU
dA:dT
Flagelin
LTx
f
WT
Nlrp3 −/−
Pycard −/−
Casp1 −/− Casp11 −/−
Ac-YVAD:
Lys
Sup

Figure 2

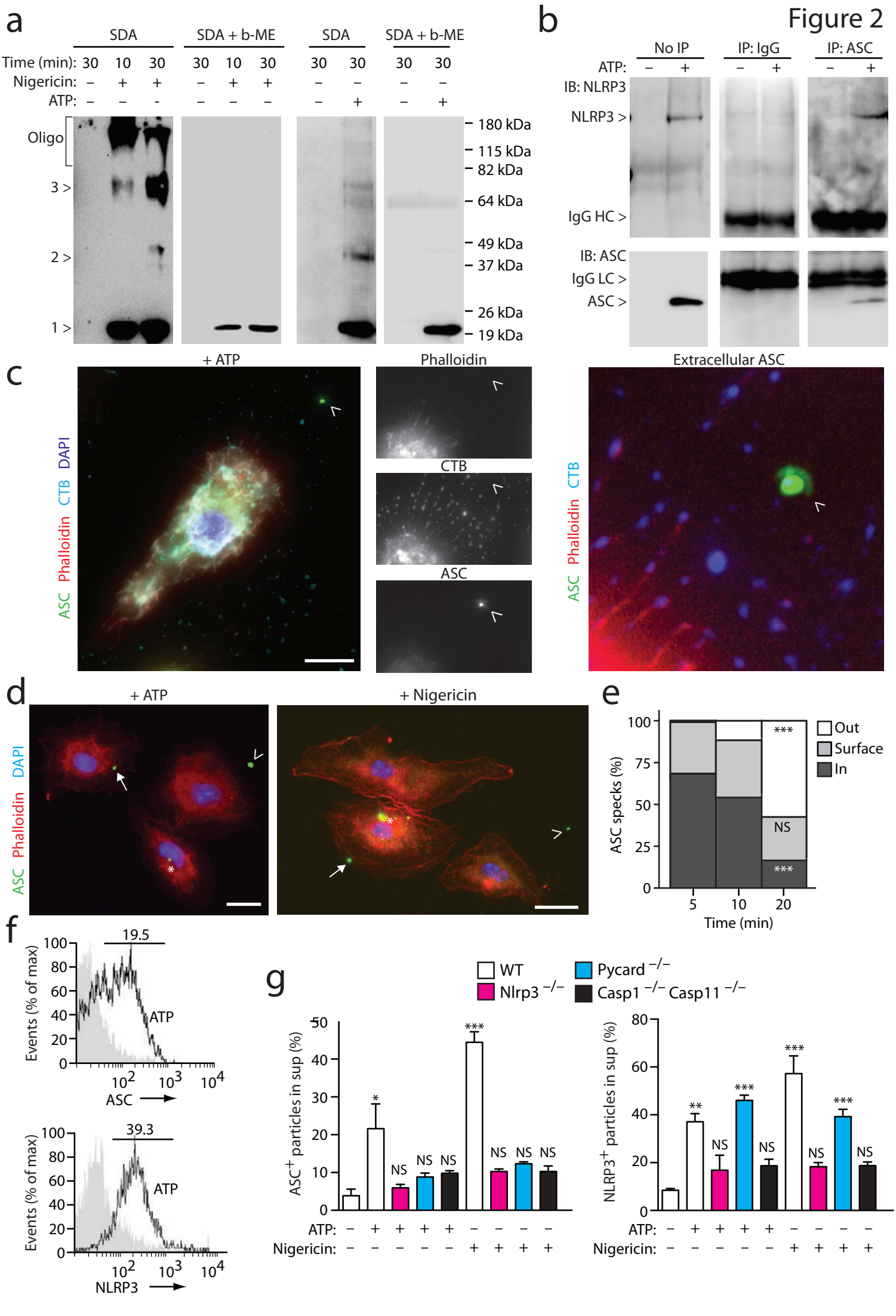
a
SDA
SDA + b-ME
SDA
SDA + b-ME
Time (min): 30 10 30 30 10 30 30 30 30 30
Nigericin: – + + – + + – – – –
ATP: – – - – – – – + – +
Oligo
3 >
2 >
1 >
180 kDa
115 kDa
82 kDa
64 kDa
49 kDa
37 kDa
26 kDa
19 kDa
b
No IP
IP: IgG
IP: ASC
ATP: – + – + – +
IB: NLRP3
NLRP3 >
IgG HC >
IB: ASC
IgG LC >
ASC >
c
+ ATP
Phalloidin
CTB
ASC
DAPI
Extracellular ASC
d
+ ATP
+ Nigericin
e
ASC specks (%)
Time (min)
Out
Surface
In
***
NS
f
19.5
ATP
Events (% of max)
ASC
39.3
NLRP3
g
WT
Nlrp3 −/−
Pycard −/−
Casp1 −/− Casp11 −/−
ASC+ particles in sup (%)
NLRP3+ particles in sup (%)
ATP:
Nigericin:

Figure 3

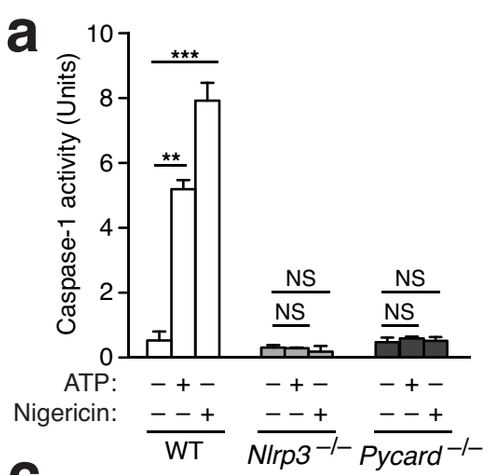
a
Caspase-1 activity (Units)
10
8
6
4
2
0
***
**
NS
NS
NS
NS
ATP: – + – – + – – + –
Nigericin: – – + – – + – – +
WT
Nlrp3 –/–
Pycard –/–

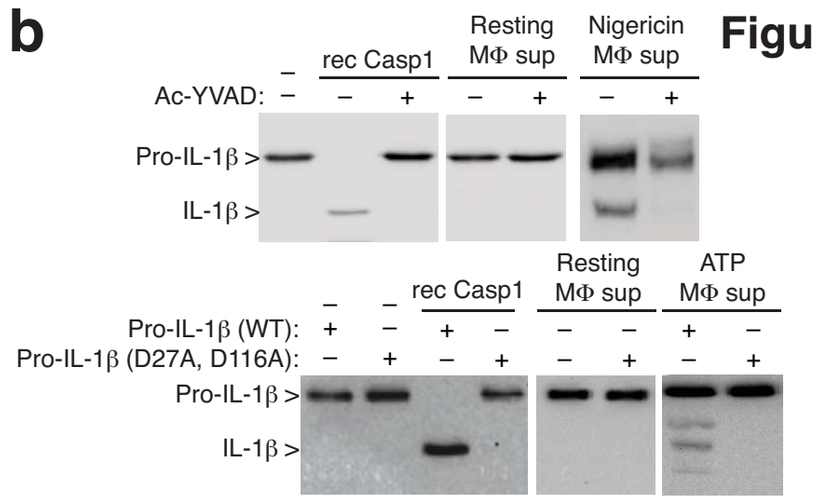
b
rec Casp1
Resting MΦ sup
Nigericin MΦ sup
Ac-YVAD: – – + – + – +
Pro-IL-1β >
IL-1β >
rec Casp1
Resting MΦ sup
ATP MΦ sup
Pro-IL-1β (WT): + – + – – – + –
Pro-IL-1β (D27A, D116A): – + – + – + – +
Pro-IL-1β >
IL-1β >

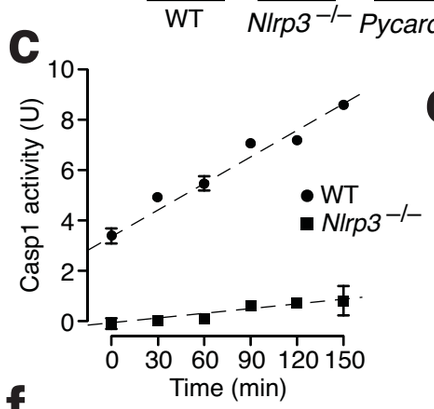
c
Casp1 activity (U)
10
8
6
4
2
0
WT
Nlrp3 –/–
0 30 60 90 120 150
Time (min)

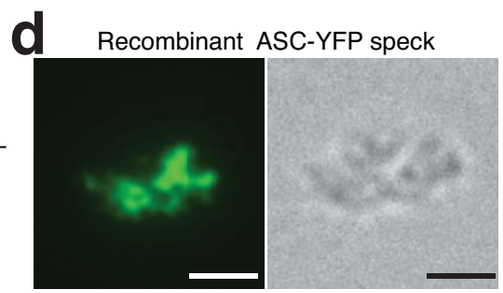
d
Recombinant ASC-YFP speck

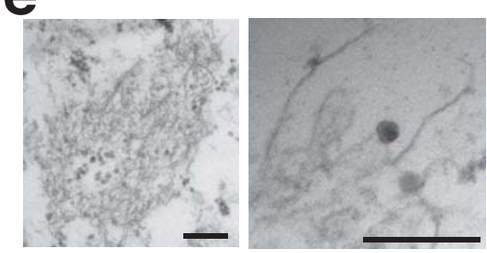
e

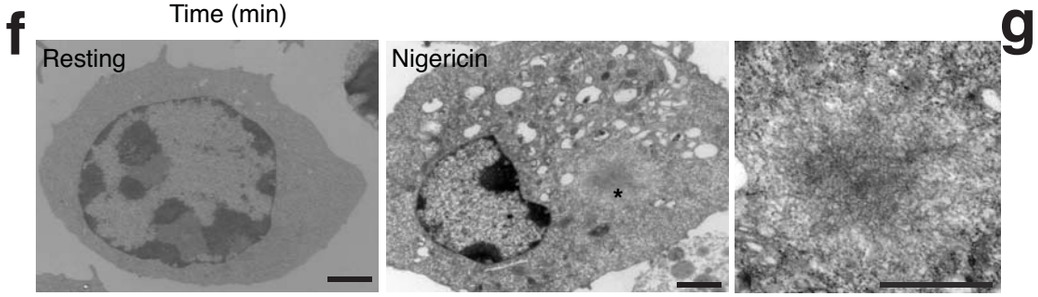
f
Resting
Nigericin
*

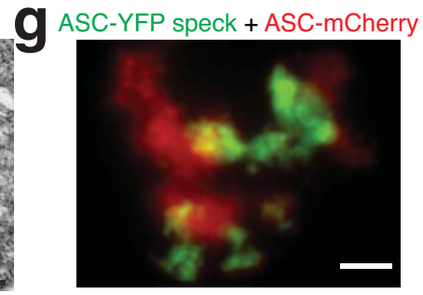
g
ASC-YFP speck + ASC-mCherry

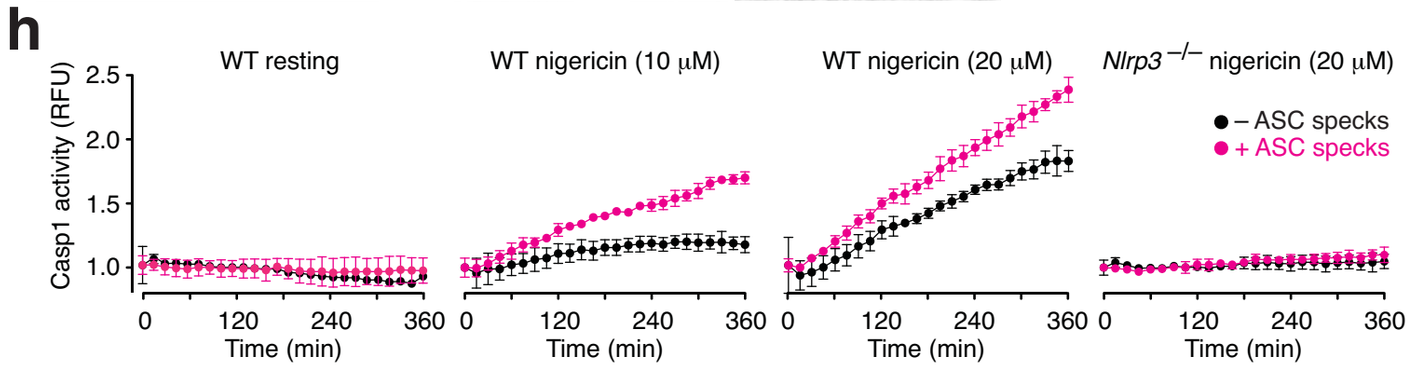
h
WT resting
WT nigericin (10 μM)
WT nigericin (20 μM)
Nlrp3 –/– nigericin (20 μM)
Casp1 activity (RFU)
2.5
2.0
1.5
1.0
– ASC specks
+ ASC specks
0 120 240 360
Time (min)

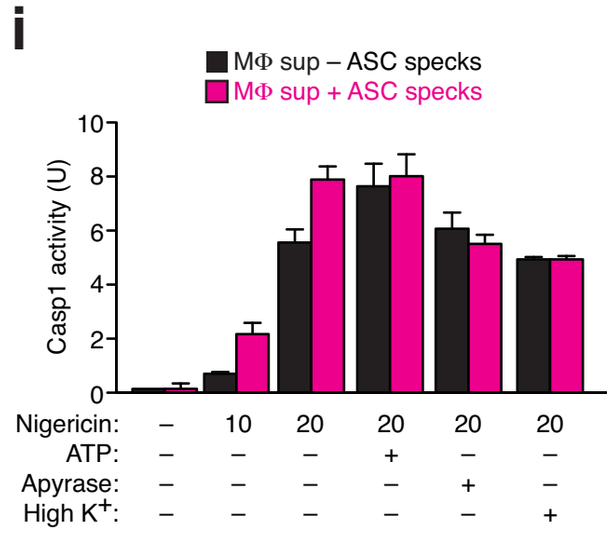
i
MΦ sup – ASC specks
MΦ sup + ASC specks
Casp1 activity (U)
10
8
6
4
2
0
Nigericin: – 10 20 20 20 20
ATP: – – – + – –
Apyrase: – – – – + –
High K+: – – – – – +

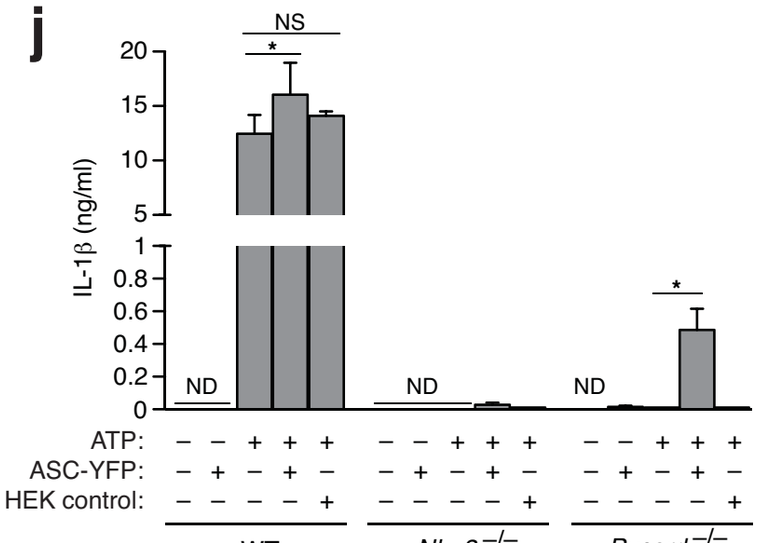
j
IL-1β (ng/ml)
20
15
10
5
1
0.8
0.6
0.4
0.2
0
NS
*
*
ND
ND
ND
ATP: – – + + + – – + + + – – + + +
ASC-YFP: – + – + – – + – + – – + – + –
HEK control: – – – – + – – – – + – – – – +
WT
Nlrp3 –/–
Pycard –/–

Figure 4

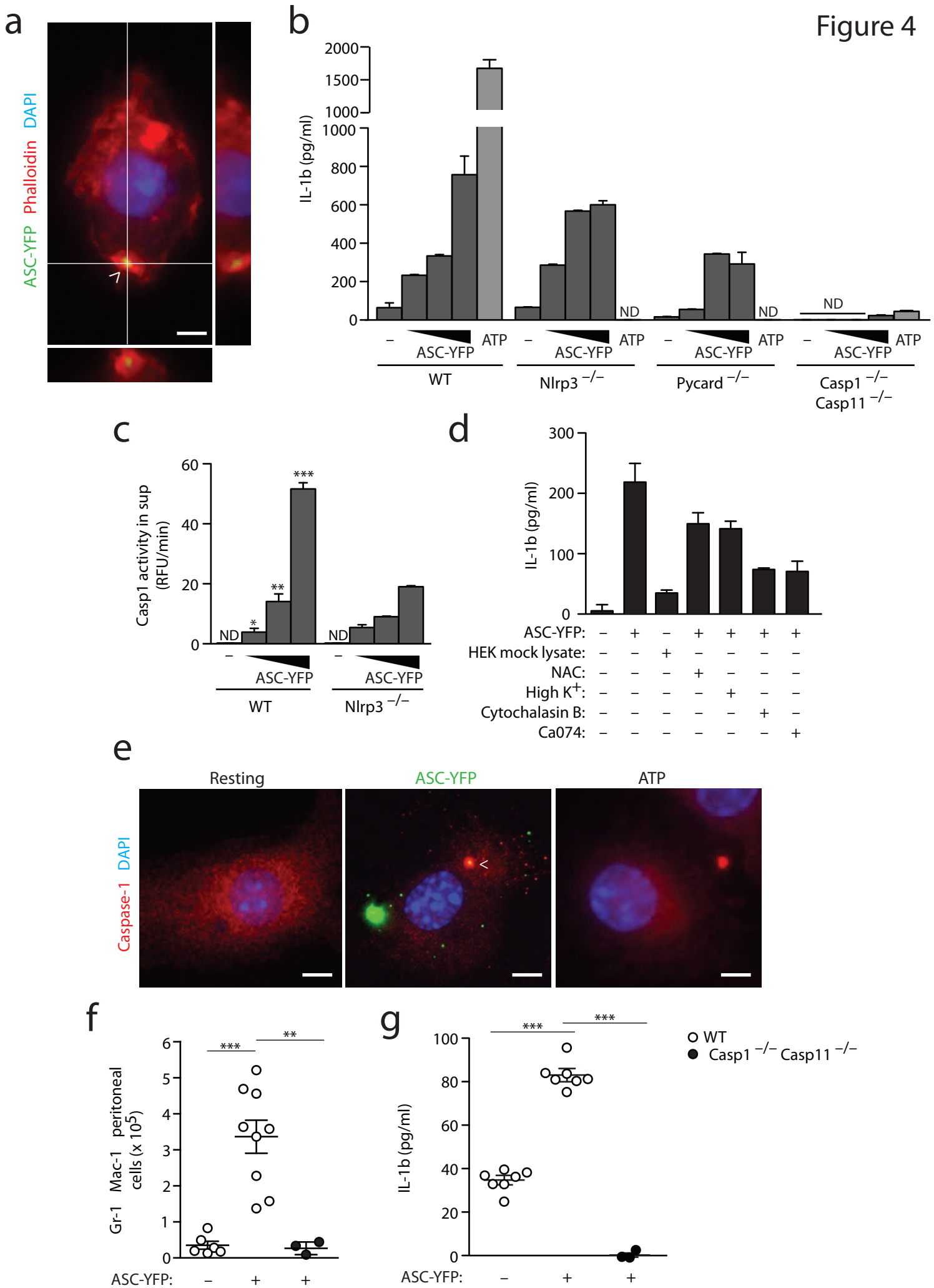
a
ASC-YFP Phalloidin DAPI
b
IL-1b (pg/ml)
2000
1500
1000
1000
800
600
400
200
0
ND
ND
ND
– ASC-YFP ATP
WT
Nlrp3 −/−
Pycard −/−
Casp1 −/−
Casp11 −/−
c
Casp1 activity in sup (RFU/min)
60
40
20
0
ND
*
**
***
ND
ASC-YFP
WT
Nlrp3 −/−
d
IL-1b (pg/ml)
300
200
100
0
ASC-YFP:
HEK mock lysate:
NAC:
High K+:
Cytochalasin B:
Ca074:
e
Resting
ASC-YFP
ATP
Caspase-1 DAPI
f
Gr-1 Mac-1 peritoneal cells (x 10^5)
6
5
4
3
2
1
0
***
**
ASC-YFP:
g
IL-1b (pg/ml)
100
80
60
40
20
0
***
***
WT
Casp1 −/− Casp11 −/−
ASC-YFP:

Figure 5

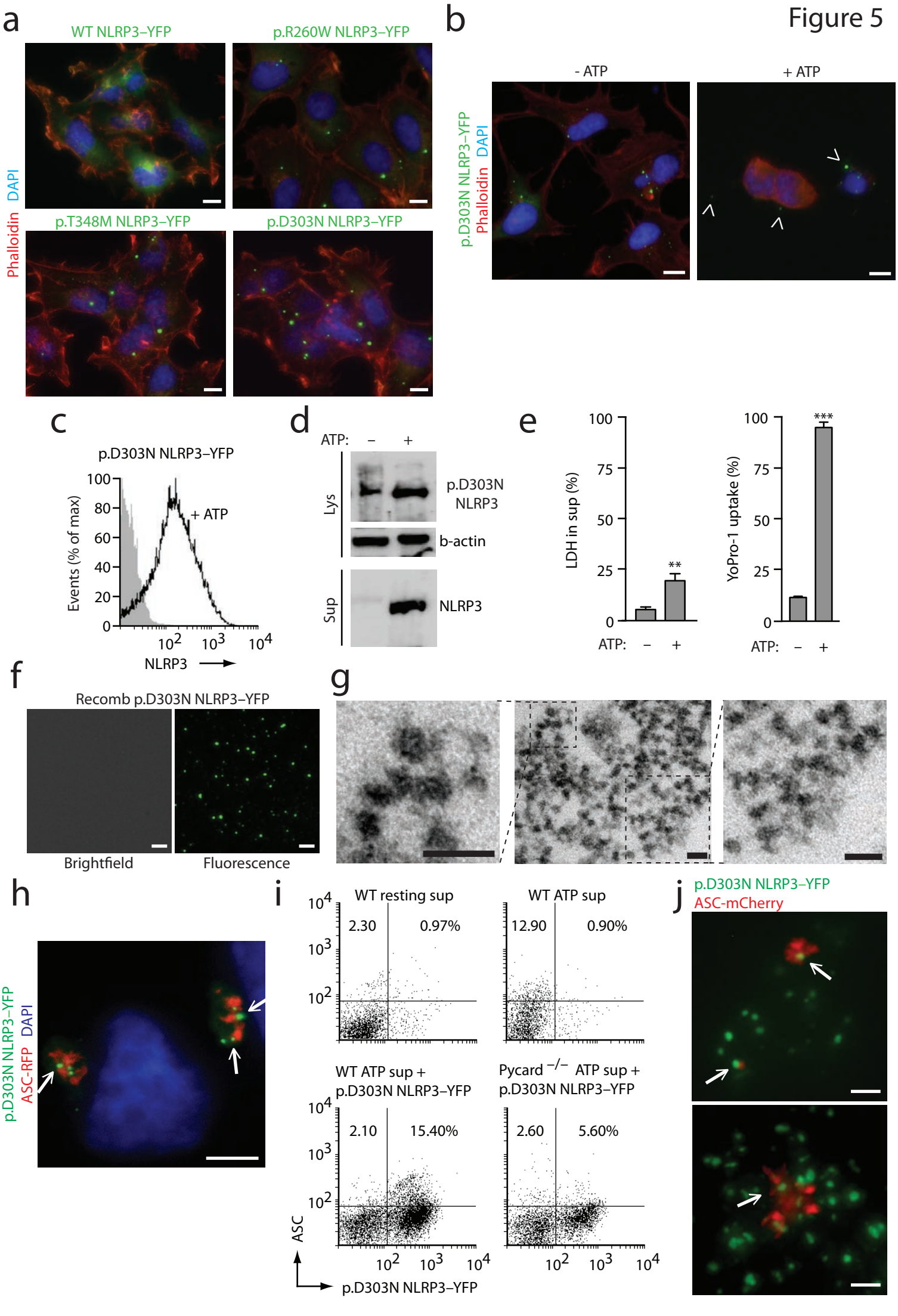
a
WT NLRP3–YFP
p.R260W NLRP3–YFP
p.T348M NLRP3–YFP
p.D303N NLRP3–YFP
DAPI
Phalloidin
b
- ATP
+ ATP
p.D303N NLRP3–YFP
Phalloidin DAPI
c
p.D303N NLRP3–YFP
Events (% of max)
+ ATP
NLRP3
d
ATP: – +
Lys
Sup
p.D303N NLRP3
b-actin
NLRP3
e
LDH in sup (%)
YoPro-1 uptake (%)
ATP: – +
**
***
f
Recomb p.D303N NLRP3–YFP
Brightfield
Fluorescence
g
h
p.D303N NLRP3–YFP
ASC-RFP DAPI
i
WT resting sup
WT ATP sup
2.30
0.97%
12.90
0.90%
WT ATP sup +
p.D303N NLRP3–YFP
Pycard –/– ATP sup +
p.D303N NLRP3–YFP
2.10
15.40%
2.60
5.60%
ASC
p.D303N NLRP3–YFP
j
p.D303N NLRP3–YFP
ASC-mCherry

Figure 6

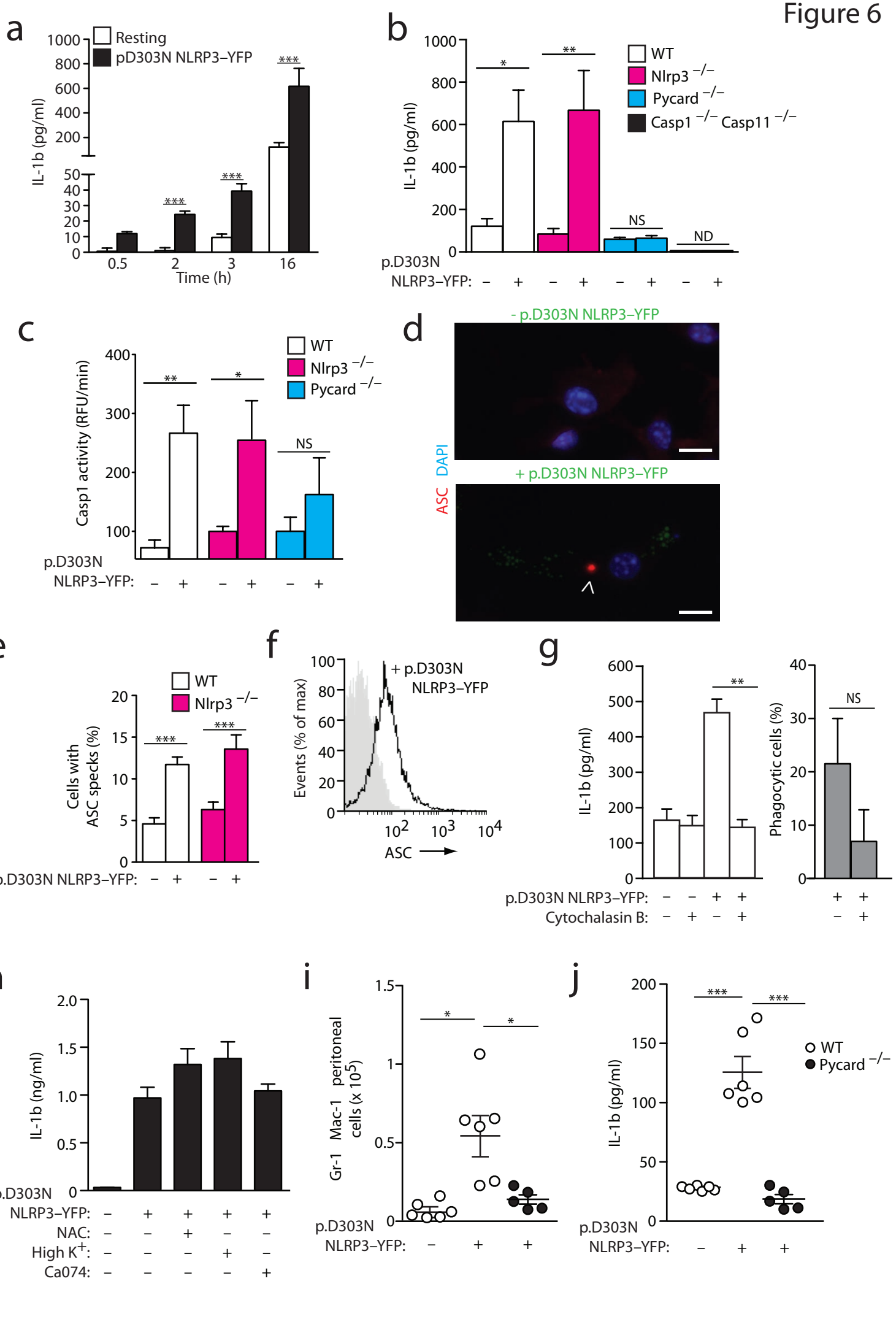
a
Resting
pD303N NLRP3–YFP
IL-1b (pg/ml)
Time (h)
b
WT
Nlrp3 −/−
Pycard −/−
Casp1 −/− Casp11 −/−
IL-1b (pg/ml)
NS
ND
p.D303N
NLRP3–YFP:
c
WT
Nlrp3 −/−
Pycard −/−
Casp1 activity (RFU/min)
NS
p.D303N
NLRP3–YFP:
d
- p.D303N NLRP3–YFP
+ p.D303N NLRP3–YFP
DAPI
ASC
e
WT
Nlrp3 −/−
Cells with ASC specks (%)
p.D303N NLRP3–YFP:
f
+ p.D303N NLRP3–YFP
Events (% of max)
ASC
g
IL-1b (pg/ml)
Phagocytic cells (%)
NS
p.D303N NLRP3–YFP:
Cytochalasin B:
h
IL-1b (ng/ml)
p.D303N
NLRP3–YFP:
NAC:
High K+:
Ca074:
i
Gr-1 Mac-1 peritoneal cells (x 10^5)
p.D303N
NLRP3–YFP:
j
WT
Pycard −/−
IL-1b (pg/ml)
p.D303N
NLRP3–YFP:

Figure 7

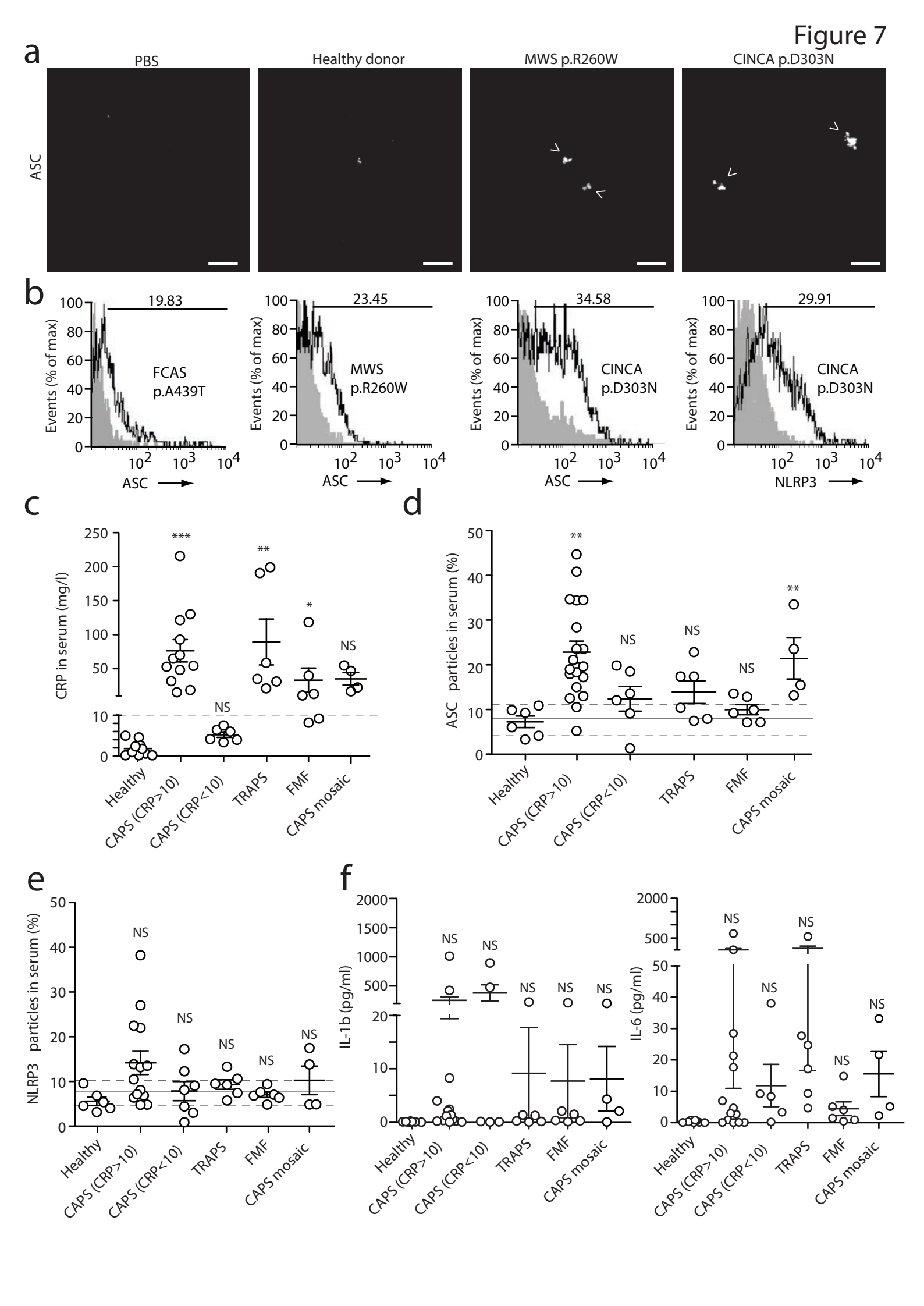
a
PBS
Healthy donor
MWS p.R260W
CINCA p.D303N
ASC
b
19.83
FCAS p.A439T
23.45
MWS p.R260W
34.58
CINCA p.D303N
29.91
CINCA p.D303N
Events (% of max)
ASC
NLRP3
c
CRP in serum (mg/l)
d
ASC particles in serum (%)
e
NLRP3 particles in serum (%)
f
IL-1b (pg/ml)
IL-6 (pg/ml)
Healthy
CAPS (CRP>10)
CAPS (CRP<10)
TRAPS
FMF
CAPS mosaic
NS